Systematic Review
http://mjiri.iums.ac.ir
Medical Journal of the Islamic Republic of Iran (MJIRI)

Med J Islam Repub Iran. 2026 (28 Sep);40.105. https://doi.org/10.47176/mjiri.40.105

Graphene Oxide and Reduced Graphene Oxide for Diabetic Wound Healing in Animal Models: A Systematic Review of Preclinical Evidence

Roya Ghafoury[1†], Afsoon Mahmoodpour[2†], Nahid Hashemi-madani[1], Zahra Emami[1*], Manizhe Ataee Kachuee[3], Mohammad E. Khamseh[1]

Received: 25 Jan 2026 Revised: 15 Sep 2026 Accepted: 25 Sep 2026 Published: 28 Sep 2026

Abstract

Background: Diabetic wounds result in significant morbidity, and current treatment options frequently yield incomplete healing. Graphene-derived nanomaterials, including GO and rGO, possess multifunctional properties that may facilitate tissue repair. This systematic review assessed animal evidence regarding their therapeutic effects and reported safety.

Methods: Following PRISMA 2020 guidelines, PubMed, Web of Science, and Scopus were searched up to March 15, 2025, for animal studies involving graphene-derived nanomaterials in diabetic full-thickness wounds. Study characteristics, outcomes, mechanisms, and safety findings were extracted. The risk of bias was assessed using SYRCLE. Due to heterogeneity, the synthesis was narrative.

Results: Twenty-three rodent studies met the inclusion criteria. GO and rGO were mainly incorporated into hydrogels, while fewer studies used scaffolds, microneedles, suspensions, or injections. Compared with untreated, vehicle, material-only, or standard-care controls, graphene-based treatments were generally associated with accelerated closure and more favorable repair markers, including collagen deposition, re-epithelialization, VEGF/CD31 expression, and reduced levels of IL-6, TNF-α, or NLRP3. Functionalized systems predominantly combined graphene with antibacterial, photothermal, nitric oxide-releasing, metal-ion, or bioactive components. SYRCLE assessment indicated a predominantly unclear risk of bias, primarily due to limited reporting of allocation concealment, random housing, and blinded outcome assessment. No significant local or systemic toxicity was reported during the short follow-up, although safety evaluation was limited.

Conclusion: Graphene-derived nanomaterials appear promising for diabetic wound repair in preclinical models. However, the evidence is limited by small-animal studies, short follow-up periods, heterogeneous formulations, and incomplete long-term biodistribution and safety assessments. Standardized preclinical studies, dose-response evaluations, and clinical trials are necessary prior to translation.

Systematic review registration: https://www.crd.york.ac.uk/PROSPERO/view/CRD420251136779

Keywords: Animal models, Diabetic wounds, Graphene oxide, Reduced graphene oxide, Hydrogels, Nanomaterials, Wound healing

This work has been published under CC BY-NC-SA 4.0 license.

Copyright© Iran University of Medical Sciences

Cite this article as: Ghafoury R, Mahmoodpour A, Hashemi-madani N, Emami Z, Ataee Kachuee M, Khamseh ME. Graphene Oxide and Reduced Graphene Oxide for Diabetic Wound Healing in Animal Models: A Systematic Review of Preclinical Evidence. *Med J Islam Repub Iran.* 2026 (28

Corresponding author: *Dr Zahra Emami, emami-z@iums.ac.ir*

† R. Ghafoury and A. Mahmoodpour contributed equally to this work.

1. Endocrine Research Center, Institute of Endocrinology and Metabolism, Iran University of Medical Sciences, Tehran, Iran
2. Endocrine Research Center, Institute of Endocrinology and Metabolism, Department of Internal Medicine, School of Medicine, Iran University of Medical Sciences, Tehran, Iran
3. Department of Radiology, Firoozgar Hospital, Iran University of Medical Sciences, Tehran, Iran

Key Messages:

↑What is "already known" in this topic:

Diabetic foot ulcers, a leading cause of amputation, often heal poorly owing to infection, impaired vascularization, and chronic inflammation. Graphene oxide (GO) and reduced GO (rGO) have antimicrobial, conductive, and scaffold-supporting properties, but their effects in diabetic wounds have not been systematically reviewed.

→What this article adds:

Across 23 rodent studies, GO- and rGO-based formulations, mainly functionalized hydrogels, were associated with faster wound closure and improved collagen deposition, re-epithelialization, angiogenesis, and infection and inflammation control. However, heterogeneous formulations, unclear risk of bias, short follow-up, and limited long-term safety data limit clinical translation.

[Downloaded from mjiri.iums.ac.ir on 2026-11-15]

[DOI: 10.47176/mjiri.40.105]

Sep);40:105. https://doi.org/10.47176/mjiri.40.105

Introduction

Diabetic foot ulcers (DFUs) constitute a serious complication of diabetes mellitus, with approximately 19%–34% of people with diabetes expected to develop a DFU at some point during their lives (1). Each year, approximately 18.6 million people develop a DFU, which precedes nearly 80% of diabetes-related lower-extremity amputations (2, 3). Despite advancements in wound care, healing remains challenging, and DFUs are associated with high rates of recurrence, amputation risk, healthcare costs, and mortality (2, 4). Impaired healing is driven by overlapping pathological processes, including persistent infection, biofilm formation, vascular insufficiency, oxidative stress, and dysregulated inflammation (5). These factors reduce oxygen and nutrient delivery, delay immune resolution, and disrupt tissue regeneration, making many diabetic wounds poorly responsive to conventional treatment (6). Consequently, therapeutic strategies that can simultaneously address infection control, inflammatory balance, angiogenesis, and tissue repair are of increasing interest.

Graphene-derived nanomaterials have been investigated as candidate platforms for wound management due to a large specific surface area, modifiable surface chemistry, and strong mechanical properties, electrical conductivity, and photothermal responsiveness (7). Both graphene oxide (GO) and reduced graphene oxide (rGO) may be incorporated into hydrogels, scaffolds, microneedles, or composite dressings to enhance local retention and interact with the wound microenvironment. Their reported effects include antibacterial activity, biofilm disruption, drug or growth-factor delivery, photothermal action under near-infrared (NIR) irradiation, and support for cell adhesion, migration, angiogenesis, and matrix deposition. However, these effects are highly dependent on material form, dose, size, oxidation state, functionalization, delivery system, and experimental model. Additionally, the biosafety of graphene-based materials remains an important translational concern, particularly regarding systemic exposure, tissue persistence, and long-term biodistribution (8-14).

Although several studies have investigated graphene-based systems for diabetic wound repair, the evidence remains fragmented across different animal models, formulations, comparators, and outcome measures. Previous reviews have addressed graphene materials in wound healing more broadly; however, a focused synthesis of their therapeutic effects and reported safety in diabetic wound models is still required. This systematic review evaluates preclinical animal evidence on graphene-derived nanomaterials for diabetic full-thickness wound healing, emphasizing formulation type, delivery system, wound-healing outcomes, proposed mechanisms, safety reporting, and risk of bias.

Methods

This systematic review was prepared in accordance with the 2020 Preferred Reporting Items for Systematic Reviews and Meta-Analyses (PRISMA) recommendations (15).

Although the protocol was developed prior to study selection, technical platform delays resulted in its retrospective registration in PROSPERO (CRD420251136779); notably, no eligibility criteria or outcomes were adjusted after the search commenced.

Eligibility Criteria

Eligibility criteria were established using the PICOS framework. Eligible studies included original preclinical animal experiments in which diabetes was either spontaneously occurring or experimentally induced, and full-thickness cutaneous wounds were created. The intervention of interest was the therapeutic application of graphene-derived nanomaterials, such as graphene itself, graphene oxide (GO), and reduced graphene oxide (rGO), or functionalized graphene-based composites. Comparators included untreated wounds, placebo or vehicle treatments, conventional wound care, standard dressings, or alternative biomaterials.

The primary outcome was wound closure, quantified as wound area reduction, percentage closure, or time to near-complete healing. Secondary outcomes included histological and molecular indicators of repair, such as re-epithelialization, collagen deposition, granulation tissue formation, angiogenesis, inflammatory cytokines, oxidative stress markers, antibacterial effects, and any reported local or systemic toxicity.

Studies were excluded if they were in vitro, ex vivo, non-mammalian, non-diabetic, or did not assess wound-healing outcomes. Additionally, studies were excluded if graphene was utilized solely as a passive carrier without evaluating its therapeutic contribution, or if the focus was mainly on material synthesis or characterization. We also excluded review articles, editorials, case reports, conference abstracts, publications written in languages other than English, and studies for which the full text was unavailable.

Search Strategy

The complete, verbatim electronic search strategies for PubMed, Scopus, and Web of Science, including all applied search terms and Boolean operators, are provided in the Appendix. The primary search strategy intentionally incorporated broader carbon-based nanomaterial terminology to maximize search sensitivity, with the predefined graphene-specific eligibility criteria subsequently applied during study screening.

Study Selection

Following database searching, all identified records were transferred to EndNote V21 for deduplication. Two reviewers separately evaluated the titles and abstracts against the established eligibility criteria. Articles consid-

[Downloaded from mjiri.iums.ac.ir on 2026-11-15]

[DOI: 10.47176/mjiri.40.105]

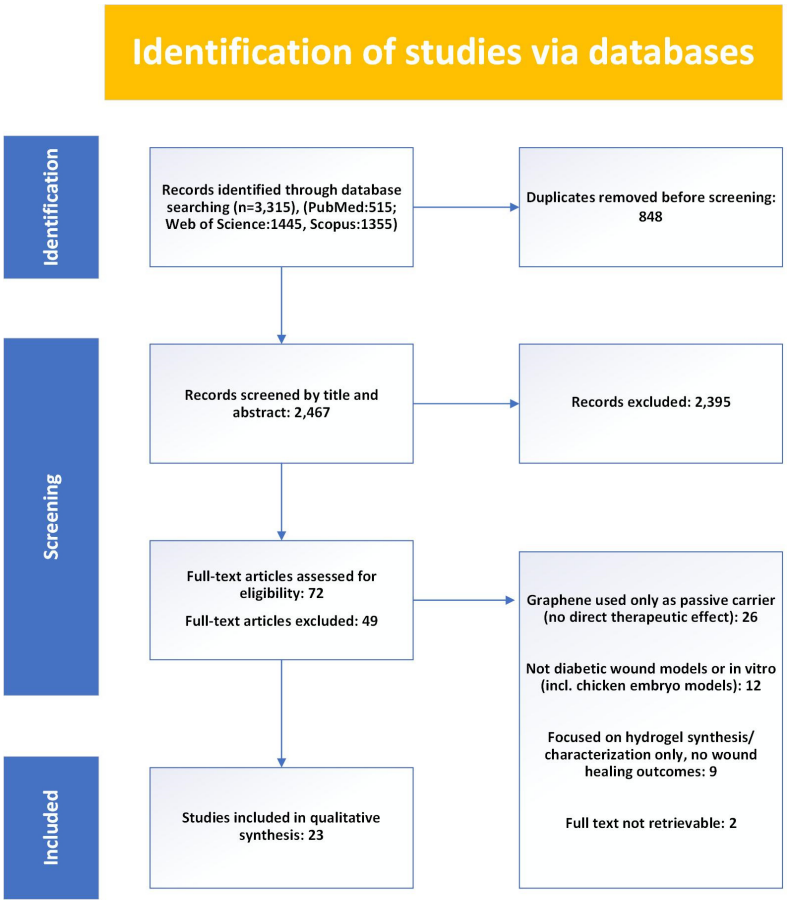


Figure 1. PRISMA flow diagram for the study selection process. Systematic searches of PubMed, Web of Science, and Scopus databases were conducted up to March 15, 2025.

ered potentially relevant proceeded to full-text review, which was also performed independently by both reviewers. Any differences in study-selection decisions were settled by discussion, with a third reviewer consulted when necessary. Figure 1 presents the complete selection procedure in a PRISMA flow diagram.

Data Extraction and Quality Assessment

Data were independently extracted by two reviewers using a standardized form. The extracted study characteristics included the author, year, animal species and strain, sex, age or weight when reported, sample size, diabetes induction method, wound type and location, graphene type, dose or concentration when reported, functionalization strategy, delivery system, co-materials, application method, treatment frequency, comparator groups, and follow-up duration.

Extracted outcomes included the percentage of wound closure, time to near-complete healing, histological findings, antibacterial effects, tested bacterial strains, angiogenic and inflammatory markers, oxidative stress findings, cytocompatibility, hemocompatibility, organ histology, serum biomarkers, biodistribution or clearance data when available, and reported adverse effects.

Two reviewers independently evaluated the methodological risk of bias in the included animal studies with the SYRCLE assessment tool (16). The evaluation covered potential biases related to study selection, performance, outcome detection, attrition, reporting, and other methodological factors. Individual domains were rated as low, high, or unclear risk of bias. Differences between the reviewers' assessments were addressed through consensus and, when required, input from a third reviewer.

Data Synthesis

Due to substantial differences among the included studies in terms of animal models, graphene formulations, delivery systems, comparators, follow-up duration, and outcome reporting, a meta-analysis was not conducted. The findings were synthesized narratively and summarized in structured tables. Study characteristics are presented in Table 1, while therapeutic outcomes, safety findings, and proposed mechanisms are summarized in Table 2.

Results

The systematic search of PubMed, Web of Science, and Scopus up to March 15, 2025, identified 3,315 records.

[Downloaded from mjiri.iums.ac.ir on 2026-11-15]

[DOI: 10.47176/mjiri.40.105]

Table 1. Characteristics of Included Preclinical Studies on Graphene-Based Nanomaterials for Diabetic Wound Repair

Author /Year	Animal population of all studied groups	Wound type	Graphene Material	Delivery System	Co-materials	Application Method and Frequency of Application	Follow up	Comparator
Thangavel P. et al., 2018	Wistar rats, ♂, diabetic model (nicotinamide 110 mg/kg + Streptozotocin (STZ) 50 mg/kg i.p.), 180–200 g, 6 groups, n = 5 per group	Full-thickness dorsal skin wound, 2 cm × 2 cm (4 cm²) diameter	Reduced graphene oxide (rGO)	Isabgol (psyllium husk), rGO nanocomposite scaffold (Isab + rGO),0.05% (w/v) rGO	Isabgol (psyllium husk polymer)	Topical, replaced every 4 days until wound closure	20 days; assessments on days 1, 4, 8, 12, 16, 20	1.sterile gauze 2. Isabgol scaffold
Beyranvand S. et al., 2019	Wistar albino rats, ♂, diabetic model (STZ 50 mg/kg i.p.), 200–250 g, 4 groups, n = 10 per group	Circular full-thickness dorsal skin wound, 2 cm diameter	Boronic acid-functionalized graphene sheets (G-BA)	Topical aqueous suspension, 50 mg/mL G BA, no scaffold/carrier	Dopamine, 2,5-thiophenediylbisboronic acid	topical, single application for 10 days	10 days; assessments on days 2, 5, 10	1. Untreated 2. 1% phenytoin cream
Tu Z. et al., 2021	C57BL/6 mice, ♂, diabetic model (STZ 110 mg/kg i.p.), 6 weeks old, 4 groups	Circular full-thickness dorsal skin wound, 10 mm diameter	Graphene oxide (GO) modified with polydopamine (GD)	Injectable, thermosensitive, self-healing conductive hydrogel (GDFE hydrogel)	F127 (Poloxamer 407), F127-ε-polylysine (F127-EPL), dopamine	Topical, Every other day until healing	21 days; assessments on days 0, 3, 7, 14, 21	1. Saline 2. FE 3. GFE
Chen X. et al., 2022	C57BL/6 mice, ♂, diabetic model (STZ-induced), 8-week-old, 30 diabetic mice (5 groups, 6 mice per group) & 6 normal control mice	Round full-thickness dorsal skin wound, 5 mm diameter	GO modified with PDLLA-PEG-PDLLA, termed PEP@GO	Thermosensitive hydrogel, 25 wt% PEP@GO	PDLLA-PEG-PDLLA triblock copolymer (PEP) (Poly-D, L-lactic acid - Polyethylene glycol - Poly-D, L-lactic acid)	Topical, Single application on Day 0	14 days; assessment on days 0, 3, 7, 10,14	1. Untreated 2. miR-21 NC 3. miR-21 mimic 4. PEP-sEVs
Ji Z. et al., 2022	BALB/C nude mice, ♀, diabetic model (STZ 150 mg/kg i.p.), 22–24 g, 4–6 weeks old, 7 groups, n = 6 per group	Full-thickness dorsal skin wound, 1.5 cm diameter	GO dispersion	GO injected intradermally along with Ad-MSCs; 0.5 mg GO co-injected with 10^7 cells, no scaffold used.	Adipose-derived mesenchymal stem cells (Ad-MSCs) with variations: untreated, Linc00324-overexpressing, or Linc00324-knockdown cells	Intradermal injection at wound margins, single injection after wound creation	14 days; Assessments on days 0, 7, 14	1. PBS injection only 2. Ad-MSCs without GO 3. Variations of Ad-MSCs with and without GO

Abbreviations: AB@MSN, ammonia borane-loaded mesoporous silica nanoparticles; Ad-MSCs, adipose-derived mesenchymal stem cells; BNN6, N,N-di-sec-butyl-N,N-dinitroso-1,4-phenylenediamine; BSA, bovine serum albumin; CTGF, connective tissue growth factor; GelMA, gelatin methacryloyl; GO, graphene oxide; GO/Co^{2+}, graphene oxide nanosheets adsorbed with cobalt ions; GO-CR, cranberry phenolic-functionalized graphene oxide; i.p., intraperitoneal; MOF-199, copper-based metal–organic framework HKUST-1; NIR, near-infrared; PBS, phosphate-buffered saline; PDA-rGO, polydopamine-reduced graphene oxide; PLA, polylactic acid; PVA, polyvinyl alcohol; PVP, polyvinylpyrrolidone; rGO, reduced graphene oxide; SD, Sprague–Dawley; STZ, streptozotocin; US, ultrasound.

[Downloaded from mjiri.iums.ac.ir on 2026-11-15]

[DOI: 10.47176/mjiri.40.105]

Table 1. Cont

Author /Year	Animal population of all studied groups	Wound type	Graphene Material	Delivery System	Co-materials	Application Method and Frequency of Application	Follow up	Comparator
Ou X. et al., 2022	Rats, ♂, diabetic model (STZ-induced), 4 groups, n = 3 /group	Full-thickness skin wound	GO	Injectable conductive hydrogel dressing (CHGB hydrogel)	N-carboxyethyl chitosan (CEC), oxidized hyaluronic acid (OHA), polymyxin B (PMB)	Topical, single injection after wound creation	18 days; assessments on days 0, 1, 3, 6, 9, 12, 15, 18	1. PBS treatment 2. CH hydrogel 3. CHG hydrogel
Wang J. et al., 2022	Diabetic full-thickness wound model, 4 groups	Full-thickness skin wound	Polydopamine- rGO	3D electrospun short fiber scaffold modified with rGO	ApF/PLCL (Electrospun polymer blend), VEGF-loaded liposomes (Lip@VEGF)	Topical, Single application on Day 0	21 days; assessments on days 0, 7, 14, 21	1.Control 2.NS scaffold 3.NS–rG scaffold
Fu X. et al., 2023	Sprague–Dawley (SD) rats, ♂, diabetic model (STZ 55 mg/kg i.p.), 6-week-old, randomly divided into 4 groups	Circular full-thickness dorsal wound, 1 cm diameter	GO nanosheets doped into gelatin/PLA short fibrous sponge (GP@GO)	Cryo-formed 3D electrospun short fibrous gelatin/PLA sponge scaffold, 0.2 mg/mL GO	Gelatin (Gel), polylactic acid (PLA), glutaraldehyde (crosslinker), glutamic acid (neutralization)	Topical, Single application on Day 0	21 days; assessment on days 0, 7, 14, 21	1. Gauze only 2. GP scaffold 3. GP@GO scaffold
He J. et al., 2023	Kunming mice, ♂, diabetic model (STZ 100 mg/kg i.p.), 4 groups.	Full-thickness skin wound	GO loaded with BNN6 (GO-BNN6, abbreviated as GB)	Injectable self-healing hydrogel (CMCS-THB-Cu-GB hydrogel), 2 mg/mL GB	Carboxymethyl chitosan (CMCS), 2,3,4-trihydroxybenzaldehyde (THB), copper chloride ($CuCl_2$), N, N-di-sec-butyl-N, N-dinitroso-1,4-phenylenediamine (BNN6)	Topical hydrogel once; Near-infrared (NIR) laser (808 nm, ~50°C) used intermittently to trigger effects, frequency not explicitly stated	21 days; Assessments on days 5, 10, 21	1. Tegaderm™ film 2.CMCS/THB/Cu/GB0 (no GB) hydrogel 3.CMCS/THB/Cu/GB2 (with GB) hydrogel
Teng L. et al., 2023	SD rats, diabetic model (STZ-induced), 8 groups, n = 4 per group	Full-thickness skin wound	GO	Injectable hybrid hydrogel (HDGS), 0.5% GO	Poly (L-glutamic acid) derivatives: PGA-SNO (S-nitrosothiol modified), PGA-DA (catechol modified)	Topical, single injection after wound creation; 4× mild NIR irradiation (808 nm, 1 W/cm², 10 min per session)	14 days; assessments on days 0, 7, 14	1. Untreated 2. Fibrin glue 3. Tegaderm 4. HD 5. HDG

[Downloaded from mjiri.iums.ac.ir on 2026-11-15]

[DOI: 10.47176/mjiri.40.105]

Table 1. Cont

Author /Year	Animal population of all studied groups	Wound type	Graphene Material	Delivery System	Co-materials	Application Method and Frequency of Application	Follow up	Comparator
Zhou J. et al., 2023	ICR mice, diabetic model (STZ-induced), 6 groups	Circular full-thickness skin wound, 8 mm diameter	GO nanosheets	Injectable, photo-crosslinked GelMA hydrogel loaded with GO and Metformin-encapsulated MSNs (MGO@GM hydrogel)	Metformin-loaded mesoporous silica nanospheres (Met@MSNs), Gelatin methacrylate (GelMA), Lithium phenyl-2,4,6-trimethylbenzoylphosphinate (LAP)	Topical, single injection after wound creation; photo-crosslinked in situ with 405 nm UV; NIR irradiation (808 nm, 1 W/cm², 200 s).	14 days; assessments on days 0, 1, 3, 7, 10, 14	1.Control (saline) 2.NIR only 3.GO@GM hydrogel 4.GO@GM + NIR
Elhabal S. et al., 2024	Albino rats, ♂, diabetic model (STZ 60 mg/kg i.p.); 8–12-week-old, 180–200 g; n = 9 per group.	Excisional dorsal wound, 4 cm × 2 mm deep	Electrochemically exfoliated GO functionalized with cranberry phenolics (GO-CR)	Thermosensitive PVA/Chitosan hydrogel cross-linked with boric acid, 0.08 % w/v GO-CR	Polyvinyl alcohol (PVA), chitosan (CH), boric acid	Topical, daily for 14 days	14 days; assessment on days 0, 3, 7, 14	1. untreated 2. Mebo & gentamycin 3. Cranberry powder 4. GO-CR alone
He J. et al., 2024	Kunming mice, ♂, diabetic model (STZ-induced), random division into 6 groups.	Full-thickness skin wound	β-cyclodextrin-reduced graphene oxide (rGB) loaded with NO donor BNN6	NIR and glucose stimuli-responsive multifunctional smart hydrogel, 2 mg/mL rGB	N-carboxyethyl chitosan-grafted phenylboronic acid (CECP), oxidized dextran (OD), ε-polylysine-coated manganese dioxide (MnO_2) nanosheets (EMn), and doxycycline (Dox).	Topical hydrogel dressing ± NIR laser irradiation; frequency not explicitly detailed	21 days; Assessments on days 5, 10, 21	1. Tegaderm™ film 2.CECP/OD/EMn0/rGB0 3.CECP/OD/EMn2/rGB0 4.CECP/OD/EMn2/rGB2 5.CECP/OD/EMn2/rGB2 + NIR
Li N. et al., 2024	SD rats, ♂, diabetic model (STZ 60 mg/kg i.p.L), 280–300 g, 8 weeks old, 6 groups, n = 6 per group	Full-thickness dorsal skin wound, 1.5 cm diameter	Polydopamine-rGO (PDA-rGO)	PDA-rGO chelating Cu^{2+} incorporated into chitosan-based hydrogel (PDA-rGO@Cu/CS hydrogel), 1 mg/ml PDA-rGO	Chitosan, copper ions ($CuCl_2$), glutaraldehyde (crosslinker)	Topical, every two days, NIR irradiation (808 nm, 1.5 W/cm², 10 min) for specified groups	14 days; assessments every 2 days	1. Control (PBS)
Liu W. et al., 2024	C57BL/6 mice, ♂, diabetic model (STZ 120 mg/kg i.p.), 10 weeks old, 5 groups	Full-thickness skin wound	GO	Double cross-linked hydrogel dressing (PVA/SA/GO/GSH), 2 mg/mL GO	Polyvinyl alcohol (PVA), sodium alginate (SA), glutathione (GSH), boronic acid derivatives, polyethylene glycol (PEG)	Topical, daily for 12 days	12 days; assessments on days 0, 3, 7, 12	1. Untreated 2. GSH alone 3. PVA/GO hydrogel 4. PVA/SA/GO hydrogel

[Downloaded from mjiri.iums.ac.ir on 2026-11-15]

[DOI: 10.47176/mjiri.40.105]

Table 1. Cont

Author /Year	Animal population of all studied groups	Wound type	Graphene Material	Delivery System	Co-materials	Application Method and Frequency of Application	Follow up	Comparator
Lu M. et al., 2024	BALB/c mice, ♂, diabetic model (STZ 100 mg/kg i.p.), 6–8 weeks old, 5 groups, n = 5 /group	Full-thickness dorsal skin wound, 8 mm diameter	Silane-modified GO (GM)	Self-healing hydrogel based on PVA–polylysine–gum arabic (PLGM3 hydrogel), 3.0 wt% GM	Polyvinyl alcohol (PVA), ε-polylysine (ε-PL), gum arabic (GA), borax (sodium tetraborate)	Topical, daily for 9 days; 808 nm NIR irradiation (1.6 W/cm² for 10 min) in the PLGM3 + NIR group	9 days; assessments on days 0, 3, 6, 9	1. Uninfected control 2. Control (infected, no treatment) 3. PLG hydrogel
Raza ur Rehman S. et al., 2024	SD rats, ♂, diabetic model (nicotinamide 230 mg/kg + STZ 35 mg/kg i.p.), 3 groups, n = 3 per group	Full-thickness dorsal skin wound, 10 mm diameter	rGO nanoparticles chemically conjugated to connective tissue growth factor (CTGF)	Gelatin methacryloyl (GelMA) hydrogel patches loaded with rGO/CTGF conjugate (GCR6), 0.006% w/w rGO and 0.00006% w/w CTGF in 5% GelMA hydrogel	Gelatin methacryloyl (GelMA), CTGF, Heparin	Topical, Single application on Day 0	21 days; assessments on days 0, 7, 14, 21	1. Normal saline 2. Blank GelMA hydrogel patch 3. Puracol Plus-Ag+
Tao H. et al., 2024	db-/db- diabetic mice, 5 groups, n=6 for wound healing model; n=3 for infected wound model	Circular full-thickness skin wound, 10 mm diameter	GO nanosheets, adsorbed with Co^{2+} ions (GO/Co^{2+})	Microneedle patch: PVP needles with AB@MSN (100 mg AB@MSN/1 mL PVP), PVA backing with GO/Co^{2+} (5 mg GO/Co^{2+}/2 mL PVA)	Ammonia borane-loaded mesoporous silica nanoparticles (AB@MSN), polyvinyl alcohol (PVA), polyvinylpyrrolidone (PVP)	Topical, single injection after wound creation; NIR irradiation (808 nm, 1.0 W/cm²) applied to infected wound groups.	12 days; assessments on days 0, 3, 7, 10, 12 (non-infected), and days 0, 4, 9 (infected)	1. No treatment 2. MSN-GO-MN 3. AB@MSN-GO-MN 4. MSN-GO/Co^{2+}-MN
Yu Z. et al., 2024	Type I diabetic rats, 4 groups, n = 6 per group	Full-thickness skin wounds	GO	MOF-199/GO nanocomposite applied directly as a drug material; Combined with dressings: chitosan, CMC, alginate, TRH; 5 wt% GO.	MOF-199 (HKUST-1), a copper-based metal-organic framework	Topical, Every two days	10 days; assessments on days 0, 2, 4, 6, 8, 10	1.MOF-199 2. GO 3. HEGFG

[Downloaded from mjiri.iums.ac.ir on 2026-11-15]

[DOI: 10.47176/mjiri.40.105]

Table 1. Cont

Author /Year	Animal population of all studied groups	Wound type	Graphene Material	Delivery System	Co-materials	Application Method and Frequency of Application	Follow up	Comparator
Zheng C. et al., 2024	SD rats, ♂, diabetic model (STZ 1% i.p.), 4 groups, n = 3 per group	Circular full-thickness dorsal skin wound, 8 mm diameter	GO functionalized with β-cyclodextrin (GO-CD) nanosheets	In situ forming supramolecular hydrogel (HA/GCA/Fe^{2+}-GOx gel); 17.5 μg/mL GO-CD	Hyaluronic acid methacrylate (HAMA), β-cyclodextrin (β-CD), Adamantane derivative (Ada), $FeSO_4$, Glucose oxidase (GOx)	Topical, Single application on Day 0; NIR irradiation (808 nm, 1 W/cm², 5 min), applied once	15 days; assessments on days 0, 3, 7, 14, 15	1. PBS group 2. 3M group
Garg S. et al., 2025	SD rats, ♂, diabetic model (STZ 60 mg/kg i.p.); 3 groups	Circular Full-thickness excisional dorsal wound	Mildly reduced GO nanosheets incorporated in BSA matrix (r(GO/BSA))	Injectable 3D nanocomposite conductive hydrogel, BSA + 0.5% GO reduced by ascorbic acid	Bovine serum albumin (BSA), ascorbic acid (reduction agent)	Topical, Every other day until healing	16 days; assessments on Days 0, 3, 7, 10, 16	1. untreated 2. BSA hydrogel only
Pan G. et al., 2025	Rats, diabetic model (STZ-induced), 5 groups, n = 5 /group	Full-thickness skin wound on foot instep	Polydopamine-rGO compounded glycine-modified fullerene (GPC)	pH/glucose dual-responsive injectable hydrogel (HPCG/PFD hydrogel)	Adipic dihydrazide bifunctionalized hyaluronic acid (AHP), oxidized chondroitin sulfate (OCS), pirfenidone (PFD)	Topical, single injection after wound creation; NIR irradiation (808 nm) applied to specific groups	21 days; assessments on days 0, 3, 7, 14, 21	1. Tegaderm™ dressing 2. HPC2 3. HPCG2 4.HPCG2 + NIR
Wang F. et al., 2025	Rats, diabetic model (high-fat and high-sugar diet after STZ-induced), 5 groups, n = 3-6 per group	Full-thickness skin wound	rGO sheets	Gelatin/PVA double-crosslinked injectable hydrogel doped with piezoelectric KNN nanocrystals and rGO (KGGP hydrogel)	Gelatin, Polyvinyl Alcohol (PVA), Piezoelectric (K,Na)NbO3 (KNN) nanocrystals	Topical hydrogel once; Ultrasound irradiation (1.0 MHz, 2.5 W/cm², 50% duty cycle) applied intermittently during treatment	14 days; assessments on days 0, 3, 7, 10, 14	1.No treatment 2.GP 3.GP + US 4.GGP 5.GGP + US 6.KGP 7.KGP + US

[Downloaded from mjiri.iums.ac.ir on 2026-11-15]

[DOI: 10.47176/mjiri.40.105]

Table 2. Summary of Therapeutic Efficacy and Mechanistic Insights of Graphene-Based Nanomaterials in Preclinical Diabetic Wound Healing

Author/Year	Study groups	Wound Closure % in all groups	Nearly Complete Healing Time	Antibacterial Effects		Bacteria Tested		Cytotoxicity		Role of Graphene
				In vitro	In vivo	In vitro	In vivo	In vitro	In vivo	
Thangavel P. et al., 2018	Normal rats: sterile gauze control, Isabgol scaffold, Isabgol + rGO scaffold. Diabetic rats: sterile gauze control, Isabgol scaffold, Isabgol + rGO scaffold.	Normal wounds: Isabgol + rGO > Isabgol > control. Isabgol + rGO achieved 100% closure by day 16 and epithelialization in 16 days; control showed 63% closure by day 16 and epithelialization in 23 days. Diabetic wounds: Isabgol + rGO > Isabgol > control. Isabgol + rGO achieved 100% closure by day 20 and epithelialization in 20 days; control showed 67% closure by day 20 and epithelialization in 26 days.	Day 20	Yes	NR	S. aureus, E. coli	NR	NIH 3T3 fibroblast viability was >70% at 48 h and ~85% at 72 h; slight reduction at 24 h was attributed to cell adaptation.	No adverse effects reported.	rGO in the Isabgol scaffold was associated with improved angiogenesis, collagen synthesis/crosslinking, ROS scavenging, antibacterial activity, fibroblast attachment/proliferation, and reduced inflammation, contributing to faster healing in normal and diabetic wounds.
Beyranvand S. et al., 2019	Diabetic infected, diabetic non-infected, non-diabetic infected, and non-diabetic non-infected wounds; each received control, phenytoin, or G-BA treatment.	Wound closure at day 10 reported as control / phenytoin / G-BA: Infected diabetic: 43% / 66% / 93%. Non-infected diabetic: 28% / 69% / 96%. Infected non-diabetic: 70% / 88% / 96%. Non-infected non-diabetic: G-BA ≈ control; phenytoin showed the best closure.	Day 10	Yes	Yes	E. coli PTCC 1330, B. cereus PTCC 1556	ampicillin-resistant E. coli 1×10^5 CFU/mL	HEK293 cell viability remained >90% at ≤1 mg/mL after 12 and 24 h by MTT assay.	No adverse effects reported at 50 mg/mL.	G-BA was associated with antimicrobial activity through binding to bacterial membranes, leading to membrane disruption and colony inhibition. It also supported cell attachment and proliferation and promoted wound repair through keratinocyte migration, collagen deposition, vascularization, ECM turnover, and enhanced angiogenesis.
Tu Z. et al., 2021	Control: saline, no hydrogel. FE: F127-ε-polylysine hydrogel. GFE: GO + F127-EPL hydrogel, without polydopamine. GDFE: polydopamine-coated GO + F127-EPL multifunctional hydrogel.	Overall healing: GDFE > GFE > FE > control. At day 3, GDFE and GFE showed smaller remaining wound areas than control: 53.09% and 58.40% vs. 78.50%. At day 14, GDFE showed near-complete healing, with 9.88% wound area remaining, compared with GFE, 21.31%; FE, 24.22%; and control, 43.02%. Complete healing time was shortest with GDFE: 17.50 days vs. GFE, 20.67 days; FE, 22.33 days; and control, 25.00 days.	Day 18	Yes	NR	S. aureus, E. coli, MRSA	NR	HUVECs and NHDFs showed comparable or increased proliferation over 5 days with FE, GFE, and GDFE hydrogels; no significant cytotoxicity was observed.	No adverse effects reported with GDFE hydrogel.	GO in the GDFE hydrogel was associated with macrophage polarization toward the M2 anti-inflammatory phenotype, enhanced angiogenesis through increased VEGF secretion and endothelial migration/tube formation, improved conductivity, scaffold support for cell adhesion, and ROS scavenging. These effects, enhanced by polydopamine, contributed to faster diabetic wound healing.

Abbreviations: ADSCs, adipose-derived stem cells; BSA, bovine serum albumin; CD31, cluster of differentiation 31; CTGF, connective tissue growth factor; ECM, extracellular matrix; GO, graphene oxide; GSH, glutathione; HUVECs, human umbilical vein endothelial cells; IL, interleukin; MRSA, methicillin-resistant Staphylococcus aureus; NIR, near-infrared; NO, nitric oxide; NR, not reported; PBS, phosphate-buffered saline; PVA, polyvinyl alcohol; rGO, reduced graphene oxide; ROS, reactive oxygen species; S. aureus, Staphylococcus aureus; STZ, streptozotocin; TNF-α, tumor necrosis factor-alpha; VEGF, vascular endothelial growth factor.

[Downloaded from mjiri.iums.ac.ir on 2026-11-15]

[DOI: 10.47176/mjiri.40.105]

Table 2. Cont

Author/Year	Study groups	Wound Closure % in all groups	Nearly Complete Healing Time	Antibacterial Effects		Bacteria Tested		Cytotoxicity		Role of Graphene
				In vitro	In vivo	In vitro	In vivo	In vitro	In vivo	
Fu X. et al., 2023	Control: gauze. GP scaffold. GP@GO scaffold. GP@GO-ADSCs scaffold.	Day 7: Control, 47.4 ± 3.6%; GP@GO, 70.0 ± 2.7%; GP@GO-ADSCs, 76.0 ± 5.1%. Day 14: Control, 74.4 ± 3.1%; GP showed similar healing to control; GP@GO-ADSCs showed greater wound closure than control. Day 21: GP@GO, 89.8 ± 0.5%; GP@GO-ADSCs, 96.1 ± 1.1%; control and GP showed slower healing.	Day 21	NR	NR	NR	NR	ADSC and HUVEC viability was maintained on GP@GO2, with no cytotoxicity over 5 days by CCK-8 assay.	No adverse effects were reported with the GP@GO scaffold containing 0.2 mg/mL GO.	GO nanosheets in the GP@GO sponge were associated with maintained ADSC/HUVEC viability, activation of the MCP-1/HIF-1α/VEGF pathway, enhanced angiogenesis, collagen deposition, re-epithelialization, increased porosity, and improved exudate absorption. These effects contributed to accelerated diabetic wound healing, with GP@GO-ADSCs achieving 96.1 ± 1.1% wound closure by day 21.
He J. et al., 2023	Tegaderm™ film. CMCS/THB/Cu/GB0 hydrogel: without GB. CMCS/THB/Cu/GB2 hydrogel: with GB. CMCS/THB/Cu/GB2 + NIR hydrogel.	Day 5: Tegaderm, 23%; CMCS/THB/Cu/GB0, 31%; CMCS/THB/Cu/GB2, 47%; CMCS/THB/Cu/GB2 + NIR, 57%. Day 21: CMCS/THB/Cu/GB2 and CMCS/THB/Cu/GB2 + NIR achieved complete wound closure; Tegaderm and CMCS/THB/Cu/GB0 reached 96% and 97% closure, respectively.	Day 21	Yes	NR	S. aureus E. coli	NR	L929 cell viability remained >90% after 24 h with the hydrogel, with mostly live cells and no significant cytotoxicity.	No adverse effects were reported at the hydrogel dosage containing 2 mg/mL GB.	GO in the CMCS/THB/Cu/GB hydrogel provided NIR-responsive photothermal activity and enabled controlled NO release from BNN6. It improved hydrogel conductivity and mechanical stability, enhanced ROS scavenging and antibacterial activity, and promoted angiogenesis, collagen deposition, and VEGF expression, contributing to complete wound closure by day 21.
Teng L. et al., 2023	Control: untreated. Fibrin glue: commercial comparator. Tegaderm: commercial comparator. HD: hydrogel without GO or NO donor. HDG: hydrogel with GO only. HDG + NIR: hydrogel with GO and 1 or 4 NIR irradiations. HDGS: hydrogel with GO and NO donor. HDGS + NIR: hydrogel with GO and NO donor plus 1 or 4 NIR irradiations. HDGS + GSH: hydrogel with GO and NO donor plus glutathione.	HDGS + NIR4 > HDGS + GSH > HDGS > HDG + NIR > HD > fibrin glue / Tegaderm / control. HDGS + NIR4 showed the fastest healing, with near-complete wound closure by days 11–14. Control and commercial dressing groups healed more slowly, with less tissue regeneration and greater inflammation.	Day 14	Yes	NR	S. aureus, E. coli, MRSA	NR	L929 fibroblast viability was approximately 90% after 48 h, and the hemolysis rate was <0.5%, indicating good biocompatibility.	No adverse effects were reported with the PGA-based hydrogel containing 0.5% w/v GO.	GO in the HDGS hydrogel provided NIR-responsive mild photothermal activity, enabling controlled NO release. It also contributed to ROS scavenging, antibacterial activity, hemostasis, angiogenesis, collagen deposition, and reduced inflammation, supporting faster diabetic wound healing.
Zhou J. et al., 2023	Control: saline. NIR only. GO@GM hydrogel. GO@GM + NIR. MGO@GM hydrogel. MGO@GM + NIR.	MGO@GM + NIR > MGO@GM > GO@GM + NIR > NIR only ≈ GO@GM > control. MGO@GM + NIR showed the fastest healing, with 63% wound closure at day 7 and 92% closure at day 14. The control group showed the slowest healing and the largest wound areas.	Day 14	Yes	Yes	S. aureus E. coli	S. aureus	RAW 264.7 macrophage viability showed no significant reduction after 24–48 h, and the MGO@GM hydrogel showed a low hemolysis rate.	No adverse effects were reported with the MGO@GM hydrogel.	GO in the MGO@GM hydrogel contributed to photothermal antibacterial activity, ROS-mediated biofilm disruption, and inhibition of quorum sensing. In combination with metformin and NIR, it supported antibacterial clearance and spatiotemporal immunomodulation, contributing to faster diabetic wound healing.

[Downloaded from mjiri.iums.ac.ir on 2026-11-15]

[DOI: 10.47176/mjiri.40.105]

Table 2. Cont

Author/Year	Study groups	Wound Closure % in all groups	Nearly Complete Healing Time	Antibacterial Effects		Bacteria Tested		Cytotoxicity		Role of Graphene
				In vitro	In vivo	In vitro	In vivo	In vitro	In vivo	
Elhabal S. et al., 2024	Group I: diabetic untreated. Group II: diabetic + Mebo + gentamycin. Group III: diabetic + cranberry powder. Group IV: diabetic + GO-CR. Group V: diabetic + PVA/CH/GO-CR hydrogel.	Wound closure at days 3/7/14: Group I: 9.5 ± 0.9% / 15.5 ± 0.5% / 30.3 ± 0.94%. Group II: 30.1 ± 0.6% / 50.1 ± 0.4% / 65.3 ± 0.5%. Group III: 25.1 ± 0.9% / 41.4 ± 0.6% / 50.5 ± 0.8%. Group IV: 54.0 ± 0.9% / 89.2 ± 0.5% / 90.2 ± 0.5%. Group V: 71.2 ± 0.8% / 92.1 ± 0.8% / 98.8 ± 0.7%.	Day 14	Yes	NR	S. epidermidis, P. aeruginosa, E. coli, K. pneumoniae	NR	HaCaT viability remained >99% up to 80 µg/mL, with no cytotoxic effect.	No adverse effects were reported with 80 µg/mL PVA/CH/GO-CR hydrogel.	GO-CR in the PVA/CH hydrogel contributed to photothermal activity, antibiofilm effects, self-healing conductivity, reduced inflammatory markers, and increased VEGF-positive vessel density, supporting 98.8 ± 0.7% wound closure by day 14.
He J. et al., 2024	Tegaderm™ film: commercial control. CECP/OD/EMn0/rGB0: hydrogel base. CECP/OD/EMn2/rGB0: hydrogel + EMn. CECP/OD/EMn2/rGB2: hydrogel + EMn + rGB. CECP/OD/EMn2/rGB2 + NIR: hydrogel + EMn + rGB + NIR. Dox-CECP/OD/EMn2/rGB2 + NIR: hydrogel + EMn + rGB + Dox + NIR.	Day 5: CECP/OD/EMn2/rGB2 + NIR, 43% ≈ Dox-CECP/OD/EMn2/rGB2 + NIR, 41% > CECP/OD/EMn2/rGB2 > CECP/OD/EMn2/rGB0 > CECP/OD/EMn0/rGB0 > Tegaderm. NIR- and Dox-treated groups showed significantly higher wound closure. Day 10: CECP/OD/EMn2/rGB2 + NIR ≈ Dox-CECP/OD/EMn2/rGB2 + NIR > other hydrogel groups > Tegaderm. All hydrogel groups showed significantly smaller wound areas than Tegaderm. Day 21: All hydrogel groups achieved near-complete closure, approximately 95–100%, compared with <95% for Tegaderm. Hydrogels promoted faster and more complete healing than Tegaderm.	Day 21	Yes	Yes	S. aureus E. coli	S. aureus	L929 fibroblast viability remained >90% after 24 h with the hydrogel; LIVE/DEAD staining confirmed mostly live cells and no significant cytotoxicity.	No adverse effects were reported at hydrogel dosages containing 2 mg/mL EMn and 2 mg/mL rGB.	rGB in the hydrogel provided NIR-responsive photothermal antibacterial activity, acted as a carrier for BNN6-mediated NO release, and improved hydrogel conductivity, mechanical strength, and adhesion. Together with EMn and doxycycline, it supported ROS reduction, oxygen generation, glucose-responsive drug release, angiogenesis, and faster infected diabetic wound healing.
Li N. et al., 2024	Control: PBS. PDA-rGO/CS hydrogel. PDA-rGO1@Cu0.2/CS hydrogel. Control + NIR. PDA-rGO/CS hydrogel + NIR. PDA-rGO1@Cu0.2/CS hydrogel + NIR.	Diabetic wounds, day 14: Control, 47.70%; PDA-rGO/CS, 81.86%; PDA-rGO1@Cu0.2/CS, 87.36%; control + NIR, 51.82%; PDA-rGO/CS + NIR, 83.82%; PDA-rGO1@Cu0.2/CS + NIR, 91.57%. Infected wounds, day 10: Control, 52.01%; PDA-rGO1@Cu0.2/CS + NIR, 90.42%.	Day 14 (diabetic model), Day 10 (infected model)	Yes	Yes	S. aureus E. coli	S. aureus	3T3 fibroblast viability remained >75%, and the hemolysis rate was <3%, indicating good biocompatibility.	No adverse effects were reported with 1 mg/mL PDA-rGO.	PDA-rGO in the chitosan hydrogel enabled NIR-triggered mild photothermal antibacterial activity, improved hydrogel mechanical strength, and promoted collagen deposition and angiogenesis, contributing to faster diabetic and infected wound healing.
Liu W. et al., 2024	Control: untreated. GSH alone. PVA/GO hydrogel. PVA/SA/GO hydrogel. PVA/SA/GO/GSH hydrogel.	PVA/SA/GO/GSH > PVA/SA/GO > GSH > PVA/GO > control. PVA/SA/GO/GSH showed near-complete wound closure, approximately 98%, by day 12. The control group healed slowest, with approximately 65% closure by day 12.	Day 12	Yes	NR	S. aureus	NR	L929 fibroblast viability remained >95%, and the hemolysis rate was <1%, indicating good biocompatibility.	No adverse effects were reported at the hydrogel dosage containing 2 mg/mL GO.	GO in the PVA/SA/GO/GSH hydrogel acted as a high-surface-area carrier for glucose- and ROS-responsive glutathione release. It also improved antioxidant activity, antibacterial effects, mechanical stability, cell migration, angiogenesis, collagen deposition, and macrophage M1-to-M2 polarization, contributing to faster diabetic wound healing.

[Downloaded from mjiri.iums.ac.ir on 2026-11-15]

[DOI: 10.47176/mjiri.40.105]

Table 2. Cont

Author/Year	Study groups	Wound Closure % in all groups	Nearly Complete Healing Time	Antibacterial Effects		Bacteria Tested		Cytotoxicity		Role of Graphene
				In vitro	In vivo	In vitro	In vivo	In vitro	In vivo	
Raza ur Rehman S. et al., 2024	Negative control: normal saline, no treatment. BGel: blank GelMA hydrogel patch. GCR6 hydrogel patch: GelMA + 0.006% rGO + 0.00006% CTGF. Positive control: Puracol Plus-Ag+ standard dressing.	GCR6 > BGel ≈ positive control > negative control. GCR6 showed the fastest healing, with near-complete wound closure by day 21, 98.3 ± 1.9%. BGel and the positive control showed moderate healing, while the negative control healed slowest.	Day 21	NR	NR	NR	NR	3T3 fibroblasts, HaCaT keratinocytes, and EA.hy926 endothelial cells showed >90% viability, indicating good biocompatibility.	No adverse effects were reported with 0.006% w/w rGO.	rGO in the GCR6 hydrogel improved cell proliferation and migration, supported hydrogel stability and porous structure, and synergized with CTGF to accelerate diabetic wound closure to 98.3 ± 1.9% by day 21.
Tao H. et al., 2024	Control: no treatment. MSN-GO-MN: microneedle patch with MSN and GO, without AB or Co^{2+}. AB@MSN-GO-MN: microneedle patch with AB-loaded MSN and GO, without Co^{2+}. MSN-GO/Co^{2+}-MN: microneedle patch with MSN and GO/Co^{2+}, without AB. AB@MSN-GO/Co^{2+}-MN: full microneedle patch with AB@MSN and GO/Co^{2+}. AB@MSN-GO/Co^{2+}-MN + NIR: full microneedle patch with NIR for infected wounds.	AB@MSN-GO/Co^{2+}-MN > AB@MSN-GO-MN ≈ MSN-GO/Co^{2+}-MN > MSN-GO-MN > control. AB@MSN-GO/Co^{2+}-MN showed the fastest healing, with near-complete wound closure by day 12, 99.7 ± 0.5%. AB@MSN-GO-MN and MSN-GO/Co^{2+}-MN showed moderate healing, while MSN-GO-MN and control healed more slowly.	Day 12	Yes	Yes	S. aureus E. coli	S. aureus E. coli	L929 fibroblasts, RAW 264.7 macrophages, and HUVECs maintained >90% viability under high-glucose conditions, indicating good biocompatibility.	No adverse effects were reported with 5 mg GO/Co^{2+} per patch.	GO/Co^{2+} in the microneedle patch provided NIR-responsive photothermal antibacterial activity and controlled Co^{2+} release. In combination with AB-derived H_2, it promoted angiogenesis, macrophage M2 polarization, collagen deposition, inflammation reduction, and tissue remodeling, contributing to 99.7 ± 0.5% wound closure by day 12.
Yu Z. et al., 2024	HEGFG: human epidermal growth factor gel, positive control. MOF-199 alone. GO alone. MOF-199/GO nanocomposite.	MOF-199/GO, 96% > HEGFG, 68.7% > MOF-199 > GO. The MOF-199/GO nanocomposite showed the best wound-healing performance.	Day 10	Yes	NR	S. aureus, E. coli, MRSA	NR	L929 cell viability remained >80% at MOF-199/GO concentrations up to 150 µg/mL after 24 h, indicating good biocompatibility.	No adverse effects were reported with MOF-199/GO treatment.	GO in the MOF-199/GO nanocomposite improved MOF-199 dispersion and stability, enhanced ROS scavenging and antibacterial activity, and supported macrophage M1-to-M2 polarization, angiogenesis, collagen synthesis, and cell proliferation, contributing to 96% wound closure by day 10.
Zheng C. et al., 2024	PBS group: negative control. 3M group: positive control. HA/GCA/Fe^{2+}-GOx hydrogel. HA/GCA/Fe^{2+}-GOx + NIR hydrogel.	HA/GCA/Fe^{2+}-GOx + NIR > HA/GCA/Fe^{2+}-GOx > 3M ≈ PBS. HA/GCA/Fe^{2+}-GOx + NIR showed the fastest healing, with 90.2% wound closure at day 14. PBS showed the slowest healing, with approximately 67% wound area remaining at day 14. The 3M group was slightly better than PBS but not significantly different, while HA/GCA/Fe^{2+}-GOx without NIR improved healing compared with controls but less than the NIR-treated group.	Day 14	Yes	Yes	S. aureus E. coli	S. aureus	RS1 and L929 fibroblast viability remained >95% after 24 h, and the hemolysis rate was <5%, indicating good biocompatibility.	No adverse effects were reported with the GO-CD hydrogel.	GO-CD in the hydrogel provided NIR-responsive photothermal activity, promoted Fenton-mediated antibacterial effects, and improved hydrogel stability and mechanical strength through host–guest interactions. These effects contributed to faster infected diabetic wound healing, reaching 90.2% closure by day 14.

[Downloaded from mjiri.iums.ac.ir on 2026-11-15]

[DOI: 10.47176/mjiri.40.105]

Table 2. Cont

Author/Year	Study groups	Wound Closure % in all groups	Nearly Complete Healing Time	Antibacterial Effects		Bacteria Tested		Cytotoxicity		Role of Graphene
				In vitro	In vivo	In vitro	In vivo	In vitro	In vivo	
Garg S. et al., 2025	Control: no treatment. BSA hydrogel. r(GO/BSA) hydrogel.	r(GO/BSA) hydrogel > BSA hydrogel > control. r(GO/BSA) hydrogel showed the fastest wound closure, with near-complete healing by day 16. The control group healed slowest.	Day 16	Yes	NR	S. aureus E. coli	NR	NIH-3T3 viability remained ≥74% at concentrations up to 20 µL/mL, showing dose-dependent but acceptable biocompatibility.	No adverse effects were reported with r(GO/BSA) hydrogel containing 0.5% w/v GO.	GO nanosheets in the r(GO/BSA) hydrogel improved electrical conductivity, mechanical strength, swelling, antibacterial activity, and bioelectrical signal transmission, supporting cell migration, proliferation, and near-complete diabetic wound closure by day 16.
Pan G. et al., 2025	Control: Tegaderm™ dressing. HPC2: hydrogel base without GPC or PFD. HPCG2: hydrogel + GPC. HPCG2 + NIR: hydrogel + GPC + NIR. HPCG2/PFD + NIR: hydrogel + GPC + pirfenidone + NIR.	HPCG2/PFD + NIR > HPCG2 + NIR > HPCG2 > HPC2 > control. HPCG2/PFD + NIR showed the fastest healing, with near-complete wound closure by day 21. The control group healed slowest, with infection-related delay.	Day 21	Yes	Yes	MRSA E. coli	MRSA	L929 fibroblast viability remained >80%, and the hemolysis rate was <5%, indicating good biocompatibility.	No adverse effects were reported at the hydrogel dosage containing 2 mg/mL GPC.	rGO in the GPC-containing hydrogel improved conductivity, mechanical strength, tissue adhesion, antioxidant activity, and NIR-responsive antibacterial activity. It also supported angiogenesis and reduced inflammation, contributing to faster infected diabetic wound healing.
Wang F.et al., 2025	Control: no treatment. GP: gelatin/PVA hydrogel. GP + US: gelatin/PVA hydrogel + ultrasound. GGP: gelatin/PVA hydrogel + rGO. GGP + US: gelatin/PVA hydrogel + rGO + ultrasound. KGP: gelatin/PVA hydrogel + KNN. KGP + US: gelatin/PVA hydrogel + KNN + ultrasound. KGGP: gelatin/PVA hydrogel + KNN + rGO. KGGP + US: gelatin/PVA hydrogel + KNN + rGO + ultrasound.	KGGP + US > KGGP > GP + US > GP > control. KGGP + US showed the fastest healing, with near-complete wound closure by day 14 and 64.8% closure at day 7. The control group healed slowest, with minimal closure and delayed tissue regeneration.	Day 14	Yes	Yes	S. aureus E. coli	S. aureus	KGGP + US enhanced Schwann cell, endothelial cell, and fibroblast viability, indicating good biocompatibility.	No adverse effects were reported with KGGP hydrogel.	rGO in the KGGP hydrogel improved electrical conductivity, charge transfer, mechanical strength, and self-healing. In combination with KNN and ultrasound, it supported piezoelectric stimulation, angiogenesis-related gene expression, neurovascular regeneration, and accelerated diabetic wound healing.

[Downloaded from mjiri.iums.ac.ir on 2026-11-15]

[DOI: 10.47176/mjiri.40.105]

After the removal of 848 duplicates in EndNote V21, 2,467 records underwent title and abstract screening.

Of these, 2,395 were excluded for reasons including a lack of focus on diabetic wounds, involvement of non-animal models, absence of graphene-based interventions, or discussion of unrelated topics. Seventy-two full-text articles were assessed for eligibility, of which 49 were excluded. The primary reasons for full-text exclusion included the use of graphene solely as a passive carrier without evaluation of its therapeutic contribution (n = 26), in vitro or non-diabetic models, including chicken embryos (n = 12), focus on hydrogel synthesis or characterization without wound-healing outcomes (n = 9), and inaccessible full text (n = 2). Ultimately, 23 animal studies evaluating graphene-derived nanomaterials for diabetic wound healing were included (17-39) (Figure 1).

The 23 included studies were published between 2018 and 2025 and were conducted exclusively in rodent models of diabetic full-thickness wounds. Most studies utilized streptozotocin-induced diabetes, while one used a genetic db/db mouse model, and another did not clearly specify the method of diabetes induction. Wounds were typically full-thickness excisional defects created on the dorsal skin, with reported sizes ranging from 5 mm to 2 cm. Fol-

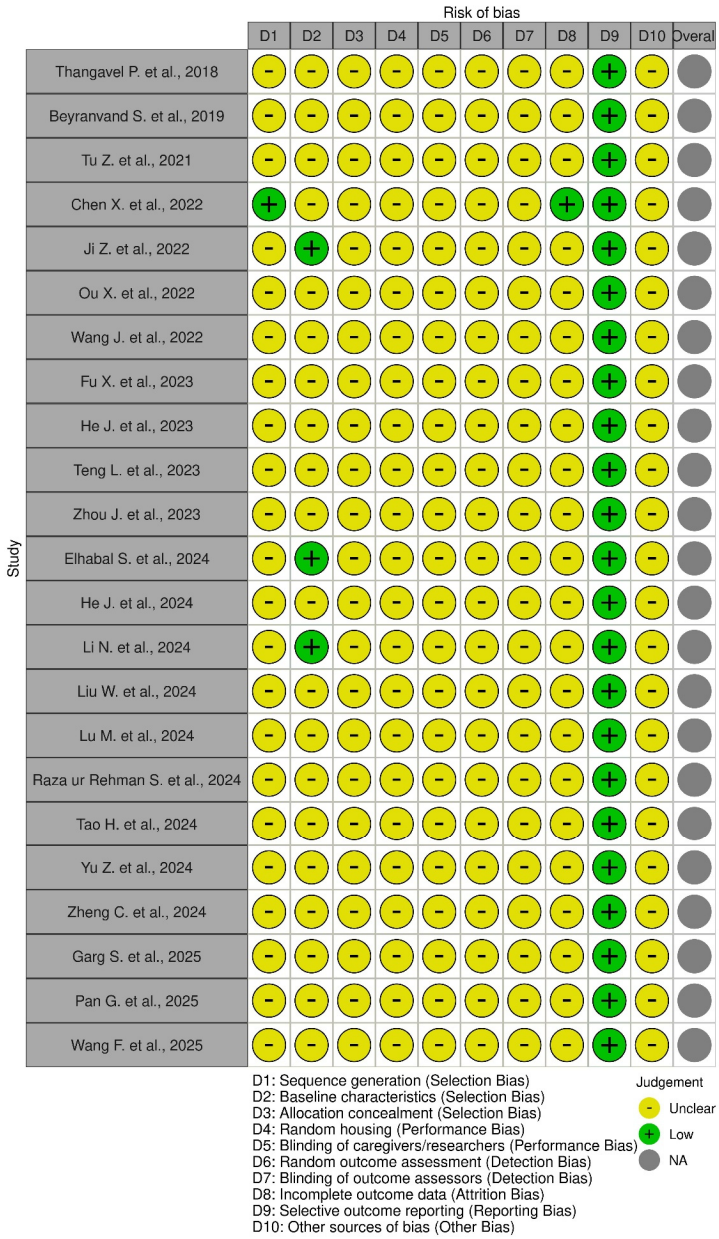


Figure 2. Risk of Bias Assessment for Included Animal Studies Using the SYRCLE Tool: Domain-Level Evaluation by Individual Study. Overall, per-study judgments are marked not applicable, as SYRCLE's risk-of-bias tool does not define a method for combining domain-level assessments into a single score.

[Downloaded from mjiri.iums.ac.ir on 2026-11-15]

[DOI: 10.47176/mjiri.40.105]

low-up durations ranged from 9 to 21 days, and treatment was generally applied topically. Comparator groups were heterogeneous, comprising untreated or gauze-treated wounds, saline/PBS controls, blank hydrogels or scaffolds, and commercial or standard-care products. Table 1 provides a detailed overview of the characteristics of the studies included. Graphene-derived materials were delivered using various platforms, most commonly hydrogels, which included injectable, thermosensitive, conductive, self-healing, and stimuli-responsive systems. Less frequently utilized delivery formats included electrospun scaffolds, microneedle patches, aqueous suspensions, and intradermal injections. Several formulations incorporated near-infrared responsiveness, typically at 808 nm, to enable photothermal activity or controlled release. Common co-materials included PVA, chitosan, gelatin, polyethylene glycol, NO donors, metal ions, growth factors, and mesenchymal stem cells. A comprehensive summary of graphene materials, co-components, delivery systems, application methods, and follow-up durations is provided in Table 1.

Methodological quality was assessed using the SYRCLE risk-of-bias tool, which evaluates ten domains of internal validity (Figures 2 and 3). Overall, most studies were judged to have an unclear risk of bias across several domains, primarily due to insufficient reporting of key methodological details. Procedures related to sequence randomization, concealment of group allocation, randomized animal housing, masking of caregivers or investigators, blinded evaluation of outcomes, and random selection for outcome assessment were generally not described. Baseline comparability was reported in only a minority of studies (21, 28, 30), and incomplete outcome data were often not clearly addressed. In contrast, selective reporting and other potential sources of bias were generally assessed as low risk, and no study was rated as high risk in any domain. These unclear ratings should be interpreted primarily as limitations in reporting rather than definitive evidence of flawed study conduct. Nevertheless, the limited reporting of randomization, allocation concealment, housing, and blinding diminishes confidence in the precision of the reported effect sizes, particularly for macroscopic wound-closure outcomes that may be susceptible to observer bias.

Compared with untreated, saline/PBS, blank scaffolds, hydrogels, commercial dressings, or standard-care comparator groups, graphene-based treatments generally accelerated wound closure in diabetic animal models. Near-complete or ≥90% wound closure was reported within 9–21 days across the included studies; however, healing rates varied according to the wound model, formulation, comparator, follow-up duration, and the use of external stimuli such as NIR irradiation or ultrasound. Histological and molecular findings commonly support improved tissue repair, including greater re-epithelialization, collagen deposition, granulation tissue formation, and angiogenesis. Reported molecular changes included increased expression of VEGF, CD31, or MCP-1, along with reduced concentrations of pro-inflammatory markers, including IL-6, TNF-α, IL-1β, or NLRP3, and increased IL-10 in some studies. Selected formulations also showed ROS-scavenging activity or NIR-responsive photothermal effects, which were associated with antibacterial and tissue-regenerative outcomes. Detailed study-level efficacy outcomes are summarized in Table 2.

Because of substantial heterogeneity in formulation design, delivery platforms, comparator groups, external stimulus application, follow-up durations, and outcome reporting, formal quantitative comparisons between GO and rGO systems, as well as between functionalized and unmodified graphene systems, were not feasible. Descriptively, GO-based systems were more commonly integrated into hydrogels designed for drug loading, antimicrobial activity, ROS modulation, and inflammatory control, whereas rGO-based systems were often used in conductive, photothermal, or electroactive platforms. Functionalized graphene formulations frequently showed strong effects within individual studies, particularly when functionalization enhanced photothermal responsiveness, metal-ion activity, nitric oxide release, antioxidant capacity, or improved tissue adhesion. To illustrate cases where a direct statistical comparison was reported, three studies providing an explicit p-value for the graphene-treated group versus its control are described below; these do not represent the largest effect sizes observed among the 23 included studies (Table 2). For instance, Li et al. reported that the PDA-rGO@Cu/chitosan hydrogel with NIR irradiation achieved 91.57% wound closure by Day 14, compared to 51.82% in the Control + NIR group (n=6 per group; P<0.0005) (30). Yu et al. reported 96% wound

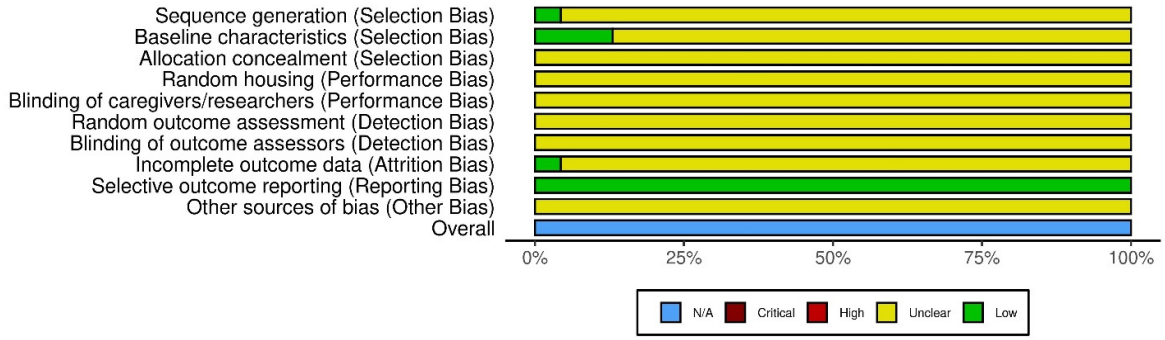


Figure 3. Summary of Risk of Bias Across Included Studies: Proportion of Studies with Low, Unclear, and High Risk by SYRCLE Domains.

[Downloaded from mjiri.iums.ac.ir on 2026-11-15]

[DOI: 10.47176/mjiri.40.105]

closure by Day 10 with MOF-199/GO nanocomposites, compared to 68.7% for the positive control gel (n=6 per group; $P<0.001$) (35). Tu et al. showed that a polydopamine-coated GO hydrogel reduced the remaining wound area to 9.88% by Day 14, compared to 43.02% in the saline control group (per-group sample size not reported; $P<0.001$) (19). Overall, the available evidence does not establish a clear superiority of GO, rGO, or any single functionalization strategy; therapeutic performance appeared to depend more on formulation design, delivery systems, and the inclusion of bioactive or stimuli-responsive components.

Antibacterial activity was evaluated in most of the included studies and reported against common wound-associated pathogens, including *Klebsiella pneumoniae*, *Bacillus cereus*, *Pseudomonas aeruginosa*, *Escherichia coli*, *Staphylococcus aureus*, and methicillin-resistant *S. aureus* (MRSA). Functionalized and stimuli-responsive systems often showed stronger antibacterial effects within individual studies, particularly when incorporating photothermal activation, metal ions, nitric oxide release, ultrasound responsiveness, or antibacterial agents. Proposed mechanisms included physical membrane disruption, ROS-mediated effects, photothermal activity, ion-

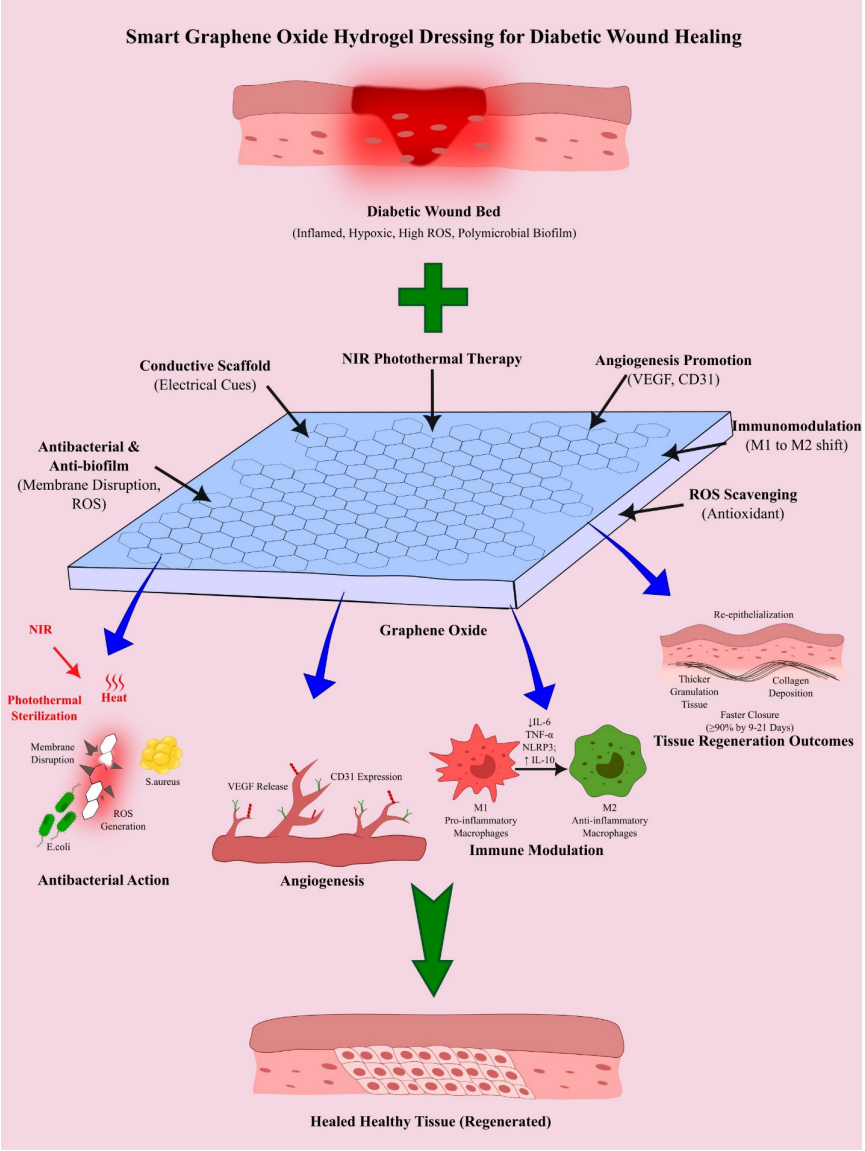


Figure 4. Schematic Illustration of Smart Graphene Oxide Hydrogel Dressing for Diabetic Wound Healing.
This diagram depicts the therapeutic mechanism of a multifunctional graphene oxide (GO) hydrogel scaffold applied to a diabetic wound bed characterized by inflammation, hypoxia, high reactive oxygen species (ROS), and polymicrobial biofilms. The central blue hexagonal lattice represents the GO hydrogel, which functions through multiple pathways: (1) Antibacterial Action, utilizing Near-Infrared (NIR) photothermal therapy and membrane disruption to neutralize bacteria like E. coli and S. aureus; (2) Angiogenesis Promotion, stimulating vascular growth factors (VEGF, CD31); (3) Immunomodulation, facilitating the transition of macrophages from the pro-inflammatory M1 phenotype to the anti-inflammatory M2 phenotype (decreasing IL-6, TNF- α α , NLRP3 while increasing IL-10); and (4) ROS Scavenging. These combined actions lead to re-epithelialization, collagen deposition, and ultimately, regenerated healthy tissue.

[Downloaded from mjiri.iums.ac.ir on 2026-11-15]

[DOI: 10.47176/mjiri.40.105]

mediated antibacterial action, and controlled release of antibacterial or nitric oxide-generating components. However, due to variations in antibacterial endpoints, tested organisms, reporting of variance, and experimental conditions across studies, the available evidence does not establish statistically confirmed superiority of any single antibacterial strategy. Short-term cytocompatibility and safety findings were generally favorable, with most studies assessing cell viability, hemocompatibility, local wound histology, or short-term major-organ histology during 9–21 days of follow-up. No significant local or systemic toxicity was reported within these short observation periods; however, serum biochemical markers, dose–response toxicity, biodistribution, degradation or clearance, scar quality, wound recurrence, and delayed inflammatory responses were rarely or not systematically evaluated.

Discussion

This systematic review synthesized preclinical evidence regarding graphene-derived nanomaterials for diabetic wound healing. Across 23 rodent studies, graphene-based formulations were generally associated with faster wound closure and improved repair markers compared to untreated, vehicle, blank-material, or standard-care controls. The most consistent benefits included enhanced re-epithelialization, collagen deposition, angiogenesis, antibacterial activity, and inflammatory modulation. These effects appear most clinically relevant when graphene is incorporated into functionalized or stimuli-responsive platforms, particularly hydrogels, which can simultaneously address several barriers to diabetic wound healing. However, the evidence remains preclinical and heterogeneous, and the apparent therapeutic promise should be interpreted alongside important limitations in study design, outcome reporting, and long-term safety assessment.

The observed benefits are biologically plausible, as graphene-based platforms can simultaneously target several impaired processes in diabetic wounds, as summarized in Figure 4. Structurally, GO- and rGO-containing hydrogels or scaffolds provide a supportive matrix for fibroblast and keratinocyte adhesion, migration, and extracellular matrix deposition, thereby contributing to granulation tissue formation, collagen deposition, and re-epithelialization (17, 18, 33, 40-42). Biologically, several formulations have been associated with reduced levels of pro-inflammatory mediators, including IL-6 and TNF-α, and increased anti-inflammatory or reparative signals such as IL-10, consistent with modulation of oxidative stress and macrophage polarization (19, 22, 23, 26, 28, 34, 35, 38, 43-46). Additionally, graphene derivatives may contribute antimicrobial activity through mechanisms such as membrane disruption, ROS-mediated bacterial injury, photothermal effects, and ion- or drug-mediated antibacterial actions (17, 22, 24, 27, 35, 36, 47-50). This combination of structural support, immune modulation, angiogenic stimulation, and infection control may elucidate why multifunctional graphene systems have been repeatedly associated with improved repair in diabetic wound models.

Previous reviews have described graphene-based materials as multifunctional platforms for wound repair, emphasizing their antimicrobial, angiogenic, regenerative, and functionalization-dependent properties (7, 8). However, these reviews did not specifically address diabetic wound models. The present review expands upon this literature by synthesizing preclinical evidence within a disease context marked by impaired angiogenesis, persistent inflammation, oxidative stress, and a heightened susceptibility to infection. This focused scope is important as the therapeutic effects observed in general wound models cannot be assumed to directly translate to diabetic wounds, where the healing process is biologically more complex and clinically more challenging.

Functionalization is a crucial determinant of therapeutic performance; however, its effects should be interpreted cautiously given the significant variability in formulations, comparators, doses, and external stimuli across studies. GO and rGO provide intrinsic properties relevant to wound repair, including high surface area, antimicrobial surface interactions, photothermal responsiveness, conductivity, and the capacity for drug or biomolecule loading (47-50). Functionalization may enhance these properties by introducing tissue adhesion, antioxidant activity, nitric oxide release, metal-ion-mediated antibacterial effects, or growth-factor delivery (22, 25, 28, 31, 51-56). The functionalization strategies employed in the included studies can be categorized into three main groups: metal or inorganic components, polymeric or organic modifications, and bioactive payloads. Metal or inorganic components were primarily utilized to enhance antibacterial and pro-angiogenic effects (34, 35). Polymeric or organic modifications were predominantly employed to improve adhesion, antioxidant activity, and biocompatibility (19, 28). Bioactive payloads were mainly incorporated to facilitate vascular maturation and tissue remodeling (23, 33). In this context, graphene was not merely a passive carrier in many formulations but rather an integral component of an active therapeutic platform. Nonetheless, the existing evidence does not conclusively demonstrate that functionalized graphene is universally superior to unmodified graphene; matched head-to-head studies are required to ascertain which modifications yield clinically meaningful benefits.

Hydrogels were the most frequently used graphene delivery systems in the included studies and appear to be the most practical platform for diabetic wound applications. Their advantages include wound-bed conformity, moisture retention, local material retention, and the ability to incorporate antimicrobial, antioxidant, pro-angiogenic, or stimuli-responsive components (42, 57-59). Other systems, including electrospun scaffolds, microneedle patches, aqueous suspensions, and intradermal injections, also showed potential but were less frequently studied. Their relative advantages remain uncertain due to the limited direct comparisons across delivery systems. Consequently, while graphene-based hydrogels appear particularly promising, future head-to-head studies are necessary to ascertain whether they provide superior therapeutic value compared to other delivery formats.

Graphene-derived materials should also be considered within the broader context of nanotechnologies for diabet-

[Downloaded from mjiri.iums.ac.ir on 2026-11-15]

[DOI: 10.47176/mjiri.40.105]

ic wound healing. Polymeric carriers, lipid-based systems, inorganic nanoparticles, metal oxides, and catalytic nanozymes have all shown potential by improving drug delivery, antimicrobial activity, angiogenesis, or oxidative-stress control (60-65). In comparison to many of these approaches, graphene platforms are distinctive due to their ability to integrate structural support, high surface area, antimicrobial surface interactions, electrical conductivity, photothermal responsiveness, and functionalization capacity within a single material system. This multifunctionality may be particularly relevant in diabetic wounds, where infection, inflammation, oxidative stress, impaired vascularization, and defective matrix remodeling coexist. However, this advantage remains largely theoretical and preclinical; direct comparative studies against established wound dressings and other nanomaterial platforms are needed before graphene-based systems can be deemed superior.

Safety findings should be regarded as an indication of short-term tolerability rather than proof of long-term biocompatibility. Most of the included studies assessed local cytocompatibility, hemocompatibility, wound-site histology, or short-term histology of major organs during follow-up periods of 9–21 days. These assessments generally did not show significant local tissue damage, hemolysis, or acute pathological changes in major organs. However, the safety evaluations were limited and inconsistent across studies. Few studies systematically examined dose–response toxicity, particle-size effects, surface-chemistry-dependent toxicity, serum biochemical markers, biodistribution, degradation, clearance, or delayed inflammatory responses after wound closure. This distinction is important because the biological behavior of graphene-family nanomaterials may vary according to flake size, oxidation state, functionalization, aggregation, dose, and route of exposure. Potential persistence or accumulation in reticuloendothelial organs such as the liver and spleen remains insufficiently characterized. Therefore, future studies should include standardized long-term nanotoxicology protocols, including serial blood chemistry, organ histology, wound-site inflammatory assessment, biodistribution tracking, and clearance evaluation. Coupled with the predominantly unclear SYRCLE ratings resulting from incomplete reporting of randomization, allocation concealment, housing, and blinding, these safety gaps indicate that the current findings should be interpreted as promising but not yet definitive.

Future Directions

To advance graphene-based nanomaterials toward clinical translation, future research should prioritize formulations that possess a clear therapeutic rationale, reproducible composition, and practical applicability in wound care. Based on current preclinical evidence, stimuli-responsive hydrogels and metal- or ion-functionalized composites appear particularly promising. Stimuli-responsive hydrogels may be advantageous due to their ability to combine wound-bed conformity, local retention, antimicrobial activity, and controlled release or photothermal activation within a single dressing platform. Similarly, metal- or ion-functionalized systems may provide value when designed to support antibacterial activity, angiogenesis, oxygen modulation, or inflammatory control. However, these approaches should be regarded as promising rather than definitively superior. Future studies should directly compare selected formulations under standardized conditions and define the optimal graphene type, dose, particle size, functionalization strategy, application frequency, and activation protocol.

Future preclinical studies must enhance methodological rigor and translational relevance. Study designs should explicitly report on randomization, allocation concealment, blinding, animal characteristics, diabetes confirmation, wound-size standardization, and predefined outcome measures. Active comparators, including standard-of-care dressings or commercially available wound products, should be included whenever possible to determine whether graphene-based formulations provide meaningful benefits beyond existing therapies. Evaluations should extend beyond early wound closure to include scar architecture, biomechanical strength, recurrence, functional skin recovery, and infection control in clinically relevant models. Long-term nanotoxicology assessments are also essential, including dose–response testing, serum biochemical markers, organ histology, biodistribution, degradation or clearance, and delayed inflammatory responses. Addressing these methodological and safety requirements will be crucial before graphene-based wound dressings can advance from promising animal studies to credible clinical evaluations.

Strengths and Limitations

This review possesses several strengths. To our knowledge, it represents the first systematic synthesis specifically focused on graphene-derived nanomaterials in diabetic wound models, a condition characterized by persistent inflammation, impaired angiogenesis, oxidative stress, susceptibility to infection, and delayed tissue repair. The review also compares unmodified and functionalized graphene systems, summarizes delivery platforms and mechanistic outcomes, and evaluates reported safety findings. Furthermore, methodological quality was assessed using the SYRCLE risk-of-bias tool, providing a structured appraisal of the reliability of preclinical evidence.

Several important constraints warrant consideration. First, all included studies were conducted using small-animal models, predominantly STZ-induced diabetic rodents, which do not fully replicate the clinical complexity of human diabetic foot ulcers; STZ alone models an insulin-deficient, type 1-like state, and only four studies (17, 33, 34, 39) used models designed to approximate type 2 diabetes. Second, most studies exhibited unclear SYRCLE risk-of-bias ratings due to incomplete reporting of randomization, allocation concealment, random housing, and blinded outcome assessment. These limitations may diminish confidence in the precision of the reported effects, particularly regarding wound-closure measurements and histological outcomes. Third, the graphene formulations were highly heterogeneous concerning GO/rGO type,

[Downloaded from mjiri.iums.ac.ir on 2026-11-15]

[DOI: 10.47176/mjiri.40.105]

functionalization, dose, delivery system, use of external stimuli, treatment frequency, and comparator groups, thereby precluding meta-analysis and limiting direct cross-study comparisons. Fourth, the follow-up periods were short, ranging from 9 to 21 days, which restricted the assessment of scar quality, recurrence, biomechanical strength, and functional skin recovery. Fifth, all 23 included studies reported favorable outcomes, and no domain was rated high risk of bias, raising the possibility of publication bias favoring positive preclinical results. Finally, safety assessments were inconsistent and primarily limited to cytocompatibility, hemocompatibility, local histology, or short-term organ histology, with limited evaluation of serum biomarkers, dose–response toxicity, biodistribution, degradation or clearance, and long-term systemic safety.

Conclusion

In conclusion, graphene-derived nanomaterials show potential as multifunctional platforms for diabetic wound healing in preclinical models, exhibiting reported antimicrobial, anti-inflammatory, angiogenic, and regenerative effects. However, the existing evidence is limited to heterogeneous small-animal studies characterized by short follow-up periods, variable methodological reporting, and incomplete long-term safety evaluations. Translating these findings to clinical practice will necessitate standardized formulation reporting, rigorous control of risk of bias, dose–response and biodistribution studies, long-term nanotoxicology assessments, and well-designed clinical trials to establish safety and efficacy in patients.

Acknowledgment

The authors acknowledge Reihane Mohammadi for providing professional illustration services for the figures.

Conflict of Interests

The authors declare that they have no competing interests.

Authors' Contributions

R. Gh. contributed to the conceptualization of the study, the development of the review protocol, the design of the database search strategy, data collection, article screening, data extraction, quality assessment, drafting of the initial manuscript, coordination of revisions, and the conceptual design of the figure.

A.M. contributed to critical revision of the manuscript for important intellectual content, substantial editing of the manuscript, and approval of the final version.

N.H.-M. contributed to independent article screening, data extraction, quality appraisal, and critical revision of the manuscript for important intellectual content.

Z.E. developed and executed the systematic search strategy, performed the database searches, managed reference organization, contributed to the review process, and critically revised the manuscript.

M.A.K. contributed to oversight of the systematic review methodology, resolution of discrepancies during study selection and data extraction, and critical revision of the manuscript for important intellectual content.

M.E.Kh. supervised the study, provided intellectual and methodological guidance, contributed to interpretation of the findings, critically revised the manuscript for important intellectual content, and approved the final version of the manuscript.

All authors reviewed and approved the final manuscript and accepted responsibility for the work, including the appropriate investigation and resolution of any concerns regarding its accuracy or integrity.

Ethical Considerations

Not applicable.

Funding Support

The study was conducted without external financial support.

Data Availability

The datasets analyzed during this review, including the full study characteristics and outcome extraction tables, are presented in Table 1 and Table 2 of this manuscript. The primary data is available from the cited publications listed in the References.

AI Use Statement

The authors declare that no AI tools were used to generate the figures, graphs, images, data, analysis, interpretation, or scientific content of this manuscript.

References

1. McDermott K, Fang M, Boulton AJ, Selvin E, Hicks CW. Etiology, epidemiology, and disparities in the burden of diabetic foot ulcers. Diabetes Care. 2023;46(1):209-21.
2. Armstrong DG, Tan T-W, Boulton AJ, Bus SA. Diabetic foot ulcers: a review. JAMA. 2023;330(1):62-75.
3. Hashempour R, MirHashemi S, Mollajafari F, Damiri S, ArabAhmadi A, Raei B. Economic burden of diabetic foot ulcer: a case of Iran. BMC Health Serv Res. 2024;24(1):363.
4. Chen L, Sun S, Gao Y, Ran X. Global mortality of diabetic foot ulcer: a systematic review and meta-analysis of observational studies. Diabetes Obes Metab. 2023;25(1):36-45.
5. Maity S, Leton N, Nayak N, Jha A, Anand N, Thompson K, et al. A systematic review of diabetic foot infections: pathogenesis, diagnosis, and management strategies. Front Clin Diabetes Healthc. 2024;5:1393309.
6. Armstrong DG, Boulton AJ, Bus SA. Diabetic foot ulcers and their recurrence. N Engl J Med. 2017;376(24):2367-75.
7. Shariati A, Hosseini SM, Chegini Z, Seifalian A, Arabestani MR. Graphene-based materials for inhibition of wound infection and accelerating wound healing. Biomed Pharmacother. 2023;158:114184.
8. Mohammed H, Kumar A, Bekyarova E, Al-Hadeethi Y, Zhang X, Chen M, et al. Antimicrobial mechanisms and effectiveness of graphene and graphene-functionalized biomaterials. A scope review. Front Bioeng Biotechnol. 2020;8:465.
9. Al-Thani RF, Patan NK, Al-Maadeed MA. Graphene oxide as antimicrobial against two gram-positive and two gram-negative bacteria in addition to one fungus. OnLine J Biol Sci. 2014;14(3):230-9.
10. Wali HF, Kareem ZH, Aldujaili NH. Antibacterial Activity of Reduced Graphene Oxide Nanoparticles Synthesized by Klebsiella Oxytoca. J Nanostruct. 2023;13(4):1150-8.
11. Wang Y, Lu Y, Zhang J, Hu X, Yang Z, Guo Y, et al. A synergistic antibacterial effect between terbium ions and reduced graphene oxide in a poly(vinyl alcohol)-alginate hydrogel for treating infected chronic wounds. J Mater Chem B. 2019;7(4):538-47.
12. Khan MUA, Razak SIA, Hassan A, Qureshi S, Stojanović GM.

[Downloaded from mjiri.iums.ac.ir on 2026-11-15]

[DOI: 10.47176/mjiri.40.105]

Multifunctional arabinoxylan-functionalized-graphene oxide based composite hydrogel for skin tissue engineering. Front Bioeng Biotechnol. 2022;10:865059.
13. Chen N, Li M, Yang J, Wang P, Song G, Wang H. Slow-sculpting graphene oxide/alginate gel loaded with platelet-rich plasma to promote wound healing in rats. Front Bioeng Biotechnol. 2024;12:1334087.
14. Zhang C, Yuan T-J, Tan M-H, Xu X-H, Huang Y-F, Peng L-H. Smart graphene-based hydrogel promotes recruitment and neural-like differentiation of bone marrow derived mesenchymal stem cells in rat skin. Biomater Sci. 2021;9(6):2146-61.
15. Page MJ, McKenzie JE, Bossuyt PM, Boutron I, Hoffmann TC, Mulrow CD, et al. The PRISMA 2020 statement: an updated guideline for reporting systematic reviews. BMJ. 2021;372:n71.
16. Hooijmans CR, Rovers MM, De Vries RB, Leenaars M, Ritskes-Hoitinga M, Langendam MW. SYRCLE's risk of bias tool for animal studies. BMC Med Res Methodol. 2014;14(1):43.
17. Thangavel P, Kannan R, Ramachandran B, Moorthy G, Suguna L, Muthuvijayan V. Development of reduced graphene oxide (rGO)-isabgol nanocomposite dressings for enhanced vascularization and accelerated wound healing in normal and diabetic rats. J Colloid Interface Sci. 2018;517:251-64.
18. Beyranvand S, Pourghobadi Z, Sattari S, Soleymani K, Donskyi I, Gharabaghi M, et al. Boronic acid functionalized graphene platforms for diabetic wound healing. Carbon. 2020;158:327-36.
19. Tu Z, Chen M, Wang M, Shao Z, Jiang X, Wang K, et al. Engineering Bioactive M2 Macrophage-Polarized Anti-Inflammatory, Antioxidant, and Antibacterial Scaffolds for Rapid Angiogenesis and Diabetic Wound Repair. Adv Funct Mater. 2021;31(30).
20. Chen X, Peng Y, Xue H, Liu G, Wang N, Shao Z. MiR-21 regulating PVT1/PTEN/IL-17 axis towards the treatment of infectious diabetic wound healing by modified GO-derived biomaterial in mouse models. J Nanobiotechnol. 2022;20(1).
21. Ji Z, Wang J, Yang S, Tao S, Shen C, Wei H, et al. Graphene oxide accelerates diabetic wound repair by inhibiting apoptosis of Ad-MSCs via Linc00324/miR-7977/STK4 pathway. FASEB J. 2022;36(11).
22. Ou X, Guan L, Guo W, Zhang X, Wu S, Guo D, et al. Graphene oxide-based injectable conductive hydrogel dressing with immunomodulatory for chronic infected diabetic wounds. Mater Des. 2022;224.
23. Wang J, Lin J, Chen L, Deng L, Cui W. Endogenous Electric-Field-Coupled Electrospun Short Fiber via Collecting Wound Exudation. Adv Mater. 2022;34(9).
24. Fu X, Wang J, Qian D, Xi L, Chen L, Du Y, et al. Oxygen Atom-Concentrating Short Fibrous Sponge Regulates Cellular Respiration for Wound Healing. Adv Fiber Mater. 2023;5(5):1773-87.
25. He J, Li Z, Wang J, Li T, Chen J, Duan X, et al. Photothermal antibacterial antioxidant conductive self-healing hydrogel with nitric oxide release accelerates diabetic wound healing. Compos Part B Eng. 2023;266.
26. Teng L, Song Y, Hu L, Bai Q, Zhang X, Dong CM. Nitric Oxide-Releasing Poly(L-glutamic acid) Hybrid Hydrogels for Accelerating Diabetic Wound Healing. Chin J Chem. 2023;41(17):2103-12.
27. Zhou J, Mei J, Liu Q, Xu D, Wang X, Zhang X, et al. Spatiotemporal On–Off Immunomodulatory Hydrogel Targeting NLRP3 Inflammasome for the Treatment of Biofilm-Infected Diabetic Wounds. Adv Funct Mater. 2023;33(12).
28. Elhabal SF, Al-Zuhairy SAS, El-Nabarawi M, Elrefai MFM, Shoela MS, Hababeh S, et al. Enhancing Photothermal Therapy for Antibiofilm Wound Healing: Insights from Graphene Oxide-Cranberry Nanosheet Loaded Hydrogel in vitro, in silico, and in vivo Evaluation. Int J Nanomed. 2024;19:12999-3027.
29. He J, Li Z, Chen J, Wang J, Qiao L, Guo B, et al. NIR/glucose stimuli-responsive multifunctional smart hydrogel wound dressing with NO/O2 dual gas-releasing property promotes infected diabetic wound healing. Chem Eng J. 2024;492.
30. Li N, Ma Q, Xu L, Wang Y, Zhang L, Jiang Y, et al. Polydopamine reduced graphene oxide/ chitosan-based hydrogel for the therapy of diabetic wound. Mater Today Commun. 2024;39.
31. Liu W, Yang Y, Li M, Mo J. Double cross-linked graphene oxide hydrogel for promoting healing of diabetic ulcers. Front Chem. 2024;12.
32. Lu M, Peng W, Kang W, Huang L, Zhang J, Tan S, et al. Self-healing hydrogel based on poly (vinyl alcohol)-poly (lysine)-gum arabic accelerates diabetic wound healing under photothermal sterilization. Int J Biol Macromol. 2024;266.
33. Raza ur Rehman S, Ullah A, Augustine R, Dalvi YB, Zahid AA, Ashammakhi N, et al. Enhanced wound healing by nanoengineered hydrogel patch loaded with connective tissue growth factor. Mater Today Commun. 2024;40.
34. Tao H, Xia Y, Tang T, Zhang Y, Qiu S, Chen J, et al. Self-responsive H2-releasing microneedle patch temporally adapts to the sequential microenvironment requirements for optimal diabetic wound healing. Chem Eng J. 2024;489.
35. Yu Z, Li M, Yang L, Liu H, Ding G, Ma S, et al. Enhancing diabetic wound healing: A two-pronged approach with ROS scavenging and ROS-independent antibacterial properties. Nano Today. 2024;57.
36. Zheng C, Wu X, Liu M, Lan Y, Liu Q, Cai E, et al. Photothermal-enhanced in situ supramolecular hydrogel promotes bacteria-infected wound healing in diabetes. Smart Med. 2024;3(1):e20230047.
37. Garg S, Tripathi S, Agrawal S, Tiwari V, Parmar AS. Nanocomposite conductive r(GO/BSA) hydrogel as an effective dressing for rapid chronic diabetic wound healing. Colloids Surf A Physicochem Eng Asp. 2025;705.
38. Pan G, Li M, Mu L, Huang Y, Liang Y, Guo B. Photothermal/Photodynamic Synergistic Antibacterial Hydrogel Dressing with pH/Glucose Dual Responsive Pirfenidone Release for Diabetic Foot Ulcers. Adv Funct Mater. 2025;35(9).
39. Wang F, Qiu J, Guan S, Chen S, Nie X, Fu Z, et al. An ultrasound-responsive hydrogel with piezoelectric-enhanced electrokinetic effect accelerates neurovascular regeneration for diabetic wound healing. Mater Today. 2025.
40. Galindo JM, San-Millán I, Castillo-Sarmiento CA, Ballesteros-Yáñez I, Herrero MA, Merino S, et al. Mimicking the extracellular matrix by incorporating functionalized graphene into hybrid hydrogels. Nanoscale. 2023;15(34):14238-48.
41. Yoon HH, Bhang SH, Kim T, Yu T, Hyeon T, Kim BS. Dual roles of graphene oxide in chondrogenic differentiation of adult stem cells: cell-adhesion substrate and growth factor-delivery carrier. Adv Funct Mater. 2014;24(41):6455-64.
42. Rehman SRu, Augustine R, Zahid AA, Ahmed R, Tariq M, Hasan A. Reduced graphene oxide incorporated GelMA hydrogel promotes angiogenesis for wound healing applications. Int J Nanomed. 2019:9603-17.
43. Qiu Y, Wang Z, Owens AC, Kulaots I, Chen Y, Kane AB, et al. Antioxidant chemistry of graphene-based materials and its role in oxidation protection technology. Nanoscale. 2014;6(20):11744-55.
44. Zhou H, Zhao K, Li W, Yang N, Liu Y, Chen C, et al. The interactions between pristine graphene and macrophages and the production of cytokines/chemokines via TLR-and NF-κB-related signaling pathways. Biomaterials. 2012;33(29):6933-42.
45. Cao X, Luo B, Mu Y, Wang C, Lu R, Yao Y, et al. The regulatory effect of TiO2 nanotubes loaded with graphene oxide on macrophage polarization in an inflammatory environment. BMC Oral Health. 2024;24(1):824.
46. Sun D, Chang Q, Lu F. Immunomodulation in diabetic wounds healing: The intersection of macrophage reprogramming and immunotherapeutic hydrogels. J Tissue Eng. 2024;15:20417314241265202.
47. Li Y, Yuan H, Von Dem Bussche A, Creighton M, Hurt RH, Kane AB, et al. Graphene microsheets enter cells through spontaneous membrane penetration at edge asperities and corner sites. Proc Natl Acad Sci U S A. 2013;110(30):12295-300.
48. He Y, Del Valle A, Qian Y, Huang Y-F. Near infrared light-mediated enhancement of reactive oxygen species generation through electron transfer from graphene oxide to iron hydroxide/oxide. Nanoscale. 2017;9(4):1559-66.
49. Xiao L, Sun J, Liu L, Hu R, Lu H, Cheng C, et al. Enhanced photothermal bactericidal activity of the reduced graphene oxide modified by cationic water-soluble conjugated polymer. ACS Appl Mater Interfaces. 2017;9(6):5382-91.
50. Li J, Wang G, Zhu H, Zhang M, Zheng X, Di Z, et al. Antibacterial activity of large-area monolayer graphene film manipulated by charge transfer. Sci Rep. 2014;4(1):4359.
51. Usman O, Ikram M, Abid N, Saeed M, Bashir A, Nabgan W, et al. Enhanced bactericidal action of rGO–ZnO hybrids prepared by the One-Pot Co-precipitation Approach. ACS Omega. 2022;7(30):26715-22.
52. Kim Y, Shin H, Jang D, Lee J, Lee Y-A, Joo SW, et al. Dual functional AgNPs-ZnO/rGO composites: Photocatalytic hydrogen

[Downloaded from mjiri.iums.ac.ir on 2026-11-15]

[DOI: 10.47176/mjiri.40.105]

production and antibacterial activity against E. coli. Appl Mater Today. 2025;42:102586.
53. Xie C, Luo J, Luo Y, Zhou J, Guo X, Lu X. Electroactive hydrogels with photothermal/photodynamic effects for effective wound healing assisted by polydopamine-modified graphene oxide. ACS Appl Mater Interfaces. 2023;15(36):42329-40.
54. Cheng J, Li C, Yang Z, Wang J, Yang P. Conductivity and interaction mechanism of polydopamine-graphene oxide: A combined experimental and density functional theory investigation. J Polym Res. 2024;31(1):22.
55. Yu Q, Shen C, Wang X, Wang Z, Liu L, Zhang J. Graphene oxide/gelatin nanofibrous scaffolds loaded with N-acetyl cysteine for promoting wound healing. Int J Nanomed. 2023:563-78.
56. Li J, Zhou C, Luo C, Qian B, Liu S, Zeng Y, et al. N-acetyl cysteine-loaded graphene oxide-collagen hybrid membrane for scarless wound healing. Theranostics. 2019;9(20):5839.
57. Ni F, Chen Y, Wang Z, Zhang X, Gao F, Shao Z, et al. Graphene derivative based hydrogels in biomedical applications. J Tissue Eng. 2024;15:20417314241282131.
58. Zhou L, Min T, Bian X, Dong Y, Zhang P, Wen Y. Rational design of intelligent and multifunctional dressing to promote acute/chronic wound healing. ACS Appl Bio Mater. 2022;5(9):4055-85.
59. Hu Y, Yu L, Dai Q, Hu X, Shen Y. Multifunctional antibacterial hydrogels for chronic wound management. Biomater Sci. 2024;12(10):2460-79.
60. Sanapalli BKR, Yele V, Singh MK, Thumbooru SN, Parvathaneni M, Karri VVSR. Human beta defensin-2 loaded PLGA nanoparticles impregnated in collagen-chitosan composite scaffold for the management of diabetic wounds. Biomed Pharmacother. 2023;161:114540.
61. Nasrullah MZ. Caffeic acid phenethyl ester loaded PEG–PLGA nanoparticles enhance wound healing in diabetic rats. Antioxidants. 2022;12(1):60.
62. Yin X, Fan X, Zhou Z, Li Q. Encapsulation of berberine decorated ZnO nano-colloids into injectable hydrogel using for diabetic wound healing. Front Chem. 2022;10:964662.
63. Zheng H, Wang X, Gao Z, Zhang X, Liu J, Yan J, et al. Chiral gold nanoparticle synergizes immunometabolic crosstalk and metabolism remodeling for diabetic wound healing. Biomaterials. 2025:123706.
64. Zgheib C, Hilton SA, Dewberry LC, Hodges MM, Ghatak S, Xu J, et al. Use of cerium oxide nanoparticles conjugated with microRNA-146a to correct the diabetic wound healing impairment. J Am Coll Surg. 2019;228(1):107-15.
65. Dai S, Yao L, Liu L, Cui J, Su Z, Zhao A, et al. Carbon dots-supported Zn single atom nanozymes for the catalytic therapy of diabetic wounds. Acta Biomater. 2024;186:454-69.

[Downloaded from mjiri.iums.ac.ir on 2026-11-15]

[DOI: 10.47176/mjiri.40.105]

Appendix

PubMed Search Strategy
(diabet*[Tiab] OR diabet* wound[Tiab] OR diabet* ulcer[Tiab] OR diabet* foot[Tiab] OR diabet* foot ulcer[Tiab] OR diabet* foot wound[Tiab] OR diabet* foot infection[Tiab] OR diabet* foot syndrome[Tiab] OR diabet* feet[Tiab] OR Diabet* skin wound[Tiab] OR Diabet* skin ulcer[Tiab] OR DFU[Tiab] OR diabetic foot[MeSH]) AND (Carbon-based nanomaterial*[Tiab] OR Carbon based nanomaterial*[Tiab] OR Carbon nanomaterial*[Tiab] OR Carbon nanostructure*[Tiab] OR Graphene[Tiab] OR Graphite [Tiab] OR graphene oxide[Tiab] OR fullerene*[Tiab] OR fullerene C60[Tiab] OR fullerene C70[Tiab] OR C60[Tiab] OR C70[Tiab] OR Single-walled carbon nanotube*[Tiab] OR Multi-walled carbon nanotube*[Tiab] OR Carbon Nanotube*[Tiab] OR NPs Nanoparticl* OR Carbon Nanofiber*[Tiab] OR Carbon Dot*[Tiab] OR Carbon Nanodot*[Tiab] OR Carbon quantum dot*[Tiab] OR Nitrogen-doped carbon dot*[Tiab] OR Graphene quantum dot*[Tiab] OR SWCNT[Tiab] OR SWNT[Tiab] OR MWCNT[Tiab] OR MWNT[Tiab] OR Graphene[MeSH] OR graphene oxide[MeSH] OR fullerenes[MeSH] OR fullerene C60 [MeSH] OR fullerene C70[MeSH Term] OR Carbon Nanotubes[MeSH])

Scopus Search Strategy
(TITLE-ABS-KEY ("diabet*" OR "diabet* wound" OR "diabet* ulcer" OR "diabet* foot" OR "diabet* foot ulcer" OR "diabet* foot wound" OR "diabet* foot infection" OR "diabet* foot syndrome" OR "diabetic feet*" OR "Diabet* skin wound" OR " Diabet* skin ulcer" OR "DFU") AND (TITLE-ABS-KEY("Carbon-based nanomaterial*" OR " Carbon nanomaterial*" OR " Carbon nanostructure*" OR "Graphene" OR "Graphite" OR "graphene oxide" OR "fullerene*" OR " fullerene C60" OR "C60" OR "fullerene C70" OR "C70" OR " Single-walled carbon nanotube*" OR "Multi-walled carbon nanotube*" OR "Carbon Nanotube*" OR " NPs Nanoparticl*" OR " Carbon Nanofiber*" OR " Carbon Dot*" OR "Carbon Nanodot*" OR " Carbon quantum dot*" OR " Nitrogen-doped carbon dot*" OR " Graphene quantum dot*" OR " SWCNT " OR "SWNT" OR "MWCNT" OR "MWNT"

Web of Science Search Strategy
TS=("diabet*" OR "diabet* wound" OR "diabet* ulcer" OR "diabet* foot" OR "diabet* foot ulcer" OR "diabet* foot wound" OR "diabet* foot infection" OR "diabet* foot syndrome" OR "diabet* feet" OR "Diabet* skin wound" OR "Diabet* skin ulcer" OR "DFU") AND TS=("Carbon-based nanomaterial*" OR "Carbon nanomaterial*" OR "Carbon nanostructure*" OR "Graphene" OR "Graphite" OR "graphene oxide" OR "fullerene*" OR "fullerene C60" OR "C60" OR "fullerene C70" OR " C70" OR "Single-walled carbon nanotube*" OR " SWCNT " OR "SWNT" OR " Multi-walled carbon nanotube*" OR "MWCNT" OR "MWNT" OR " Carbon Nanotube*" OR " NPs Nanoparticl*" OR " Carbon Nanofiber*" OR " Carbon Dot*" OR "Carbon Nanodot*" OR "Carbon quantum dot*" OR "Nitrogen-doped carbon dot*" OR " Graphene quantum dot*")

[Downloaded from mjiri.iums.ac.ir on 2026-11-15]

[DOI: 10.47176/mjiri.40.105]